

DEVELOPMENT OF A ROBUST ELECTROSTATICALLY DEFLECTING  
PRINTHEAD FOR THREE DIMENSIONAL PRINTING

by

David Brancazio

B.S. Mechanical Engineering, Massachusetts Institute of Technology, Cambridge MA

(1989)

Submitted to the Department of  
Mechanical Engineering in Partial Fulfillment of  
the Requirements for the  
Degree of

MASTER OF SCIENCE

at the

Massachusetts Institute of Technology

May 1991

© Massachusetts Institute of Technology, 1991, All rights reserved.

Signature of Author \_\_\_\_\_

Department of Mechanical Engineering  
May 10, 1991

Certified by \_\_\_\_\_

Emanuel M. Sachs  
Associate Professor, Mechanical Engineering  
Thesis Supervisor

Accepted by \_\_\_\_\_

Ain A. Sonin  
Chairman, Graduate Committee

ARCHIVES

MASSACHUSETTS INSTITUTE  
OF TECHNOLOGY

1

JUN 12 1991

LIBRARIES

# DEVELOPMENT OF A ROBUST ELECTROSTATICALLY DEFLECTING PRINthead FOR THREE DIMENSIONAL PRINTING

by

DAVID BRANCAZIO

Submitted to the Department of Mechanical Engineering  
on May 10, 1991 in partial fulfillment of the  
requirements for the Degree of Master of Science

## ABSTRACT

Three Dimensional Printing is a process for the manufacture of tooling and prototype parts directly from computer models. It functions by the deposition of powdered material in layers followed by the selective binding of the powder by "inkjet" printing of a liquid binder. An x-y positioning system is used to raster-scan a modulated nozzle over a powder bed. Following the sequential application of layers, the unbound powder is removed, resulting in a complex three-dimensional part. The process may be applied to the production of metal, ceramic, and metal-ceramic composite parts.

A printhead that selectively prints binder was developed for a prototype machine that prints parts up to three inches on a side. A continuous jet of binder is broken up into a regular sequence of droplets using piezoelectric excitation. An amplified computer signal is used to capacitively charge selected droplets as they pass through a set of closely spaced charging plates. Droplets then pass through an electric field which causes charged droplets to deflect into a droplet catcher, while uncharged droplets pass straight through to the powder bed. By synchronizing droplet charging to nozzle motion, the proper part cross-sections can be printed.

The printhead applies continuous-jet printing technology used by several companies in the ink-jet printing industry. However, to date, no industrially available printheads have been found that are suitable for Three Dimensional Printing. This results primarily from incompatibility with properties of the binder material, specifically its tendency to deposit solid residue on printhead components.

Reliability is limited chiefly by the existence of "satellite" droplets which tend to obstruct the jet, requiring that the printhead be cleaned occasionally. Techniques for the elimination of these droplets are being investigated. The design is robust to variations in the jet produced by the commercially available wire-bonding tools used as nozzles. For future machines which will use up to one hundred nozzles simultaneously, this variability will need to be greatly minimized. Electroformed nickel orifice plates are being investigated as nozzles and tested for greater repeatability. Alternate piezoelectric transducer configurations are also being investigated.

Thesis Supervisor: Dr. Emanuel Sachs

Title: Rockwell International Associate Professor of  
Mechanical Engineering

# Dedication

To my parents, who never doubted that they would one day see this document.

# Acknowledgements

I would like to acknowledge the support under the Strategic Manufacturing Initiative of the National Science Foundation as well as the MIT Leaders for Manufacturing Program, and members of the Three Dimensional Printing Consortium for their support and ideas and for giving us neat things to print.

The writing of this thesis would not have been possible, or would have been much less fun, without the following people:

Ely Sachs for looking after me these last two years. Words cannot express what a positive experience working with you has been. Thanks for keeping me off the streets, too! 3DP *INC.* is just around the bend!

Professors Michael Cima and James Cornie for their ideas and insights.

Fred Cote´ for lots of help and good ideas (although he'll never admit it) and Kevin Barron and Kevin Spratt for their help.

Alain Curodeau, Ze skating phenomenon, for finally learning to make funny jokes in English, and Beth Pruitt, Sue Perrin, and Rebecca Anderson for their help and for keeping me sane while I finished my thesis.

John Lee for hiding everything useful in the lab, and Klaus Kremmin for always trying to borrow my car.

Chris Harris, Tailin Fan, Steve Michaels and Alan Lauder for not strangling me after the printhead *still* wasn't working after three hours.

Sally Stiffler for convincing Dean Moses that Ely should hire me, Kathy Larson for tolerating me, and Denise Robbi for letting me borrow her computer on her first day here.

Jim Bredt, a fellow "printhead," for being sillier than I am and for LOTS of help on my thesis, together we shall conquer the evil satellite droplets!

My housemates Eric and Jean for being good friends and for making *my* schedule seem less bizarre.

My friends Alex, Amy, Anita, Betsy, Donna, Harald, James, Larry, Mark, Mike, Maryann, Nicole, Stacy, Warren... who hopefully understood that I didn't call because I was working...

My Aunt Vida for the inflatable dinosaur, "Alf" bedsheets, mechanical Godzilla, the Energizer "Zambunny" and other gifts that brought me fame.

My grandparents for their love and for trying to understand the research I'm doing.

To my parents, thanks for 24 years of love and support. You see, I really wasn't just playing IM sports all these years!

Diane Brongo has helped me so much that she really needs her own page. A short list includes help in brainstorming, designing the electronics, teaching me to figure skate, proofreading the manuscript, bringing me food, and rescuing Jim and I from our abysmal circuit-debugging attempts. Thanks for making grad school a far more wonderful experience than I ever dreamed!

# Contents

Acknowledgements.....	4
Contents.....	5
List of Figures.....	7
Introduction.....	9
Motivation.....	9
1.2 Three Dimensional Printing - The Current Work.....	10
1.3 Printhead Development.....	13
2. Continuous-jet Printing of Binder.....	15
2.1 Basic printhead layout and operation.....	15
2.2 Formation of discrete droplets.....	16
2.2 Capacitive charging of droplets.....	17
2.3 Droplet deflection.....	18
3. Printhead Design.....	20
3.1 Goals.....	20
3.2 Overall design.....	22
3.3 Design details.....	25
3.3.1 Nozzle assembly and mounting components.....	25
3.3.2 Piezo excitation.....	26
3.3.3 Droplet charging assembly.....	27
3.3.4 Deflection cell.....	27
3.3.5 Droplet catching and removal.....	29
3.3.6 Drive electronics.....	29
3.4 Discussion.....	31
4. Performance of Prototype.....	33
4.1 Effects of satellite droplets.....	33
4.2 Buildup on printhead components.....	34
4.3 Droplet placement error.....	34
4.4 Set-up time, startup/shutdown.....	37
4.5 Suggested improvements.....	37
5 Towards a Multiple-Nozzle Printhead.....	41
5.1 Requirements.....	41
5.2 Orifice plate configurations and experiments.....	42
5.2.1 Sources.....	42
5.2.2 Laser-drilled orifices.....	43

5.2.3 Electroformed orifices.....	45
5.3 Possible piezo configurations.....	46
5.3.1 Mechanisms for causing droplet formation .....	46
5.4 Steps to Prevent Clogging .....	48
References .....	51
Appendix 1: Piezo Operation .....	53
A1.1 Introduction.....	53
A1.2 Quantifying piezo behavior .....	54
A1.3 Mechanical deformations.....	56
Appendix 2: Charging Characteristics of Printhead and Nominal Parameters.....	59
A2.1 Charged droplet behavior in an electrostatic field .....	59
A2.2 Nominal parameter values.....	61
Appendix 3: Partial Droplet Charging .....	63
Appendix 4: Satellite Droplets.....	66
A4.1 Introduction.....	66
A4.2 Studies of satellite droplet formation.....	66
A4.2 Implications for Three Dimensional Printing .....	70
Appendix 5: Printhead Evolution .....	71
A5.1: Overall concept development.....	71
A5.2: Droplet catcher design- the continuing story.....	75
Appendix 6: Parts Drawings.....	78

# List of Figures

<u>Figure</u>	<u>Description</u>	<u>page</u>
1.1	Three Dimensional Printing machine.....	11
1.2	Sequence of operations in the Three Dimensional Printing process.....	12
1.3	A part created using Three Dimensional Printing.....	13
2.1	Schematic of continuous-jet printhead.....	16
2.2	Droplet charging with parallel plates.....	18
3.1	Exploded view of printhead.....	23
3.2	Assembled printhead.....	24
3.3	Nozzle assembly components.....	26
3.4a	Catcher configuration with combined ground plate/catcher.....	28
3.4b	Catcher configuration with independent catcher.....	28
3.5	Drive electronics for electrostatic switching.....	30
4.1	Buildup due to satellite droplets (worst case).....	34
4.2	Observed merging of charged and uncharged droplets.....	36
4.3	Breakoff length vs. stimulation frequency.....	40
5.1	Fixture for testing orifice plate.....	44
5.2	A laser-drilled hole in a .005" thick stainless steel plate.....	45
5.3	Cross-section of an electroformed hole used as a nozzle.....	45
5.4	Device to test pressure-wave stimulation of fluid jet.....	47
5.5	A resonator assembly.....	48
5.6a	Cross-flushing system using two flow sources and one pressure source.....	49
5.6b	Cross-flushing system using two flow sources.....	50
A1.1	Subscript conventions for piezo materials.....	54
A1.2	Stimulation modes for piezo motors [Piezo Systems].....	57
A2.1	Physical representation of parameters.....	61

A3.1	Response of V1 to a 40 kHz square wave input signal.....	63
A4.1	Typical rearward merging satellite droplet behavior.....	67
A4.2	Photograph of satellite droplet formation in a binder jet. ....	68
A5.1	Droplet removal system for prototype printhead.....	72
A5.2	Former printhead design.....	73



# Introduction

## Motivation

Two needs which are key to industrial productivity and competitiveness are the reduction in time to market for new products and the flexible manufacture of products in small quantities. Three Dimensional Printing targets a critical subset of the problems that must be overcome in order to achieve shorter product development cycles and flexible manufacturing for mechanical parts. The problems addressed are rapid prototyping, rapid fabrication of tooling, and the low cost manufacture of tooling.

A major contributor to the time to market for new products is the time required to fabricate prototypes. Rapid prototyping can shorten the product development cycle and improve the design process by providing rapid and effective feedback to the designer. Some applications require rapid prototyping of non-functional parts for use in assessing the aesthetic aspect of a design or the fit and assembly of a design. Other applications require functional parts. Often, it is advantageous if the functional part is fabricated by the same process that will be used in production.

A second major contributor to the time to market is the time required to develop tooling, such as molds and dies. For some types of tooling, such as injection molding dies, the turnaround time for the design and fabrication of a tool routinely extends to several months. The long lead times are due to the fact that tooling is generally one of a kind and can be extremely complex, requiring a great deal of human attention to detail.

In present practice, tooling is a gating item not only in lead time, but in manufacturing cost as well. In fact, tooling costs often determine the minimum economic batch size for a given process.

The three issues of prototyping requirements, tooling lead time, and tooling cost are related in that it is the combination of long lead times and high cost which make it impractical to fabricate preproduction prototypes by the same process that will be used in production.

As an example of the difficulties with today's technologies, consider the use of lost wax casting to produce a batch of 100 parts of a high temperature alloy in a geometry not suitable for machining. The first step is the fabrication of an aluminum die to make the wax positives. In a typical part, the tooling cost dominates the manufacturing cost, accounting for 90% of the total part cost. In addition, it would commonly take 4-10 weeks to procure the aluminum tool for the wax positives.

Current options do not provide a satisfactory solution to the demands for rapid and flexible manufacturing. The goal of Three Dimensional Printing is to produce complex three dimensional parts directly from computer models of the parts, with no part specific tooling required. This process will be used to produce both functional parts and tooling for prototypes and small batch production.

## **1.2 Three Dimensional Printing - The Current Work**

Three Dimensional Printing is a manufacturing process for the production of complex three-dimensional parts directly from a computer model of the part, with no tooling required. Three Dimensional Printing creates parts by a layered printing process. The information for each layer is obtained by applying a slicing algorithm to the computer model of the part. Parts are created inside a piston containing a powder bed. The piston is dropped several thousandths of an inch and a new layer of powder is spread across the top. The new layer is selectively joined where the part is to be formed by "ink-jet printing" binder into the powder. This is done by raster-scanning a modulating printhead over the powder bed (figure 1.1).

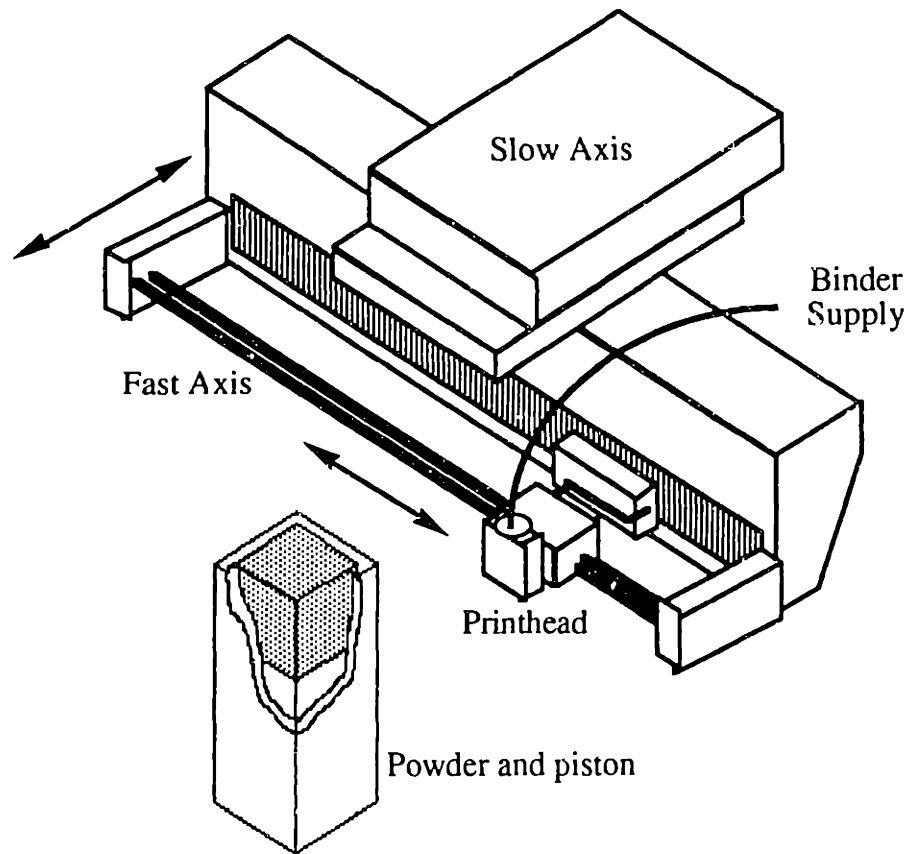


Figure 1.1: Three Dimensional Printing machine.

The printhead holds a nozzle which dispenses pressurized binder and uses a piezoelectric element to break the stream into a regular series of droplets. It then selectively deflects droplets into a "catcher" using electrostatic deflection. Deflected droplets are collected and later recycled; undeflected droplets are printed into the part being formed.

The piston is lowered and a new layer of powder is spread out and selectively joined. The layering process is repeated until the part is completely printed (figure 1.2). Following a heat treatment, the unbound powder is removed, leaving the fabricated part. A printed part is shown in figure 1.3.

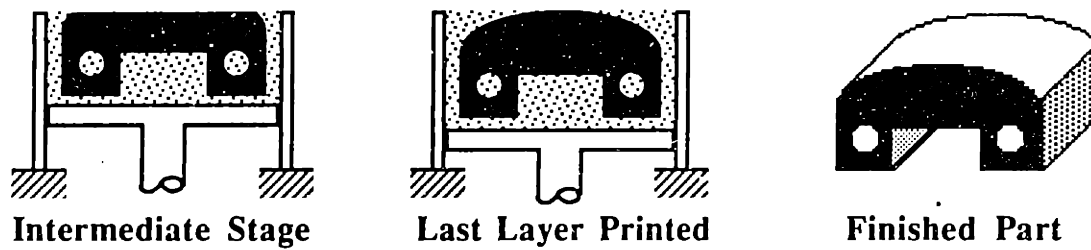
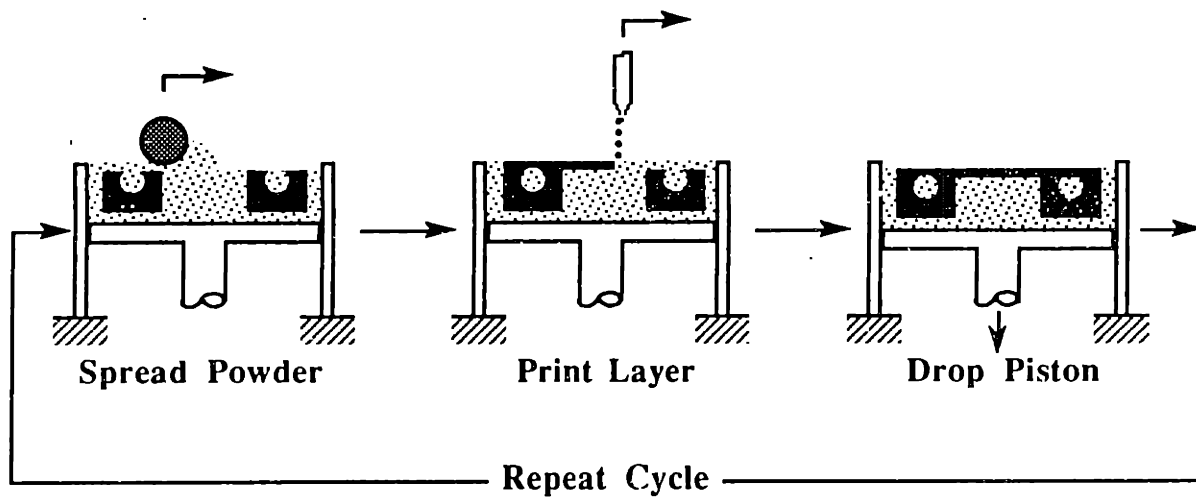


Figure 1.2. Sequence of operations in the Three Dimensional Printing process.

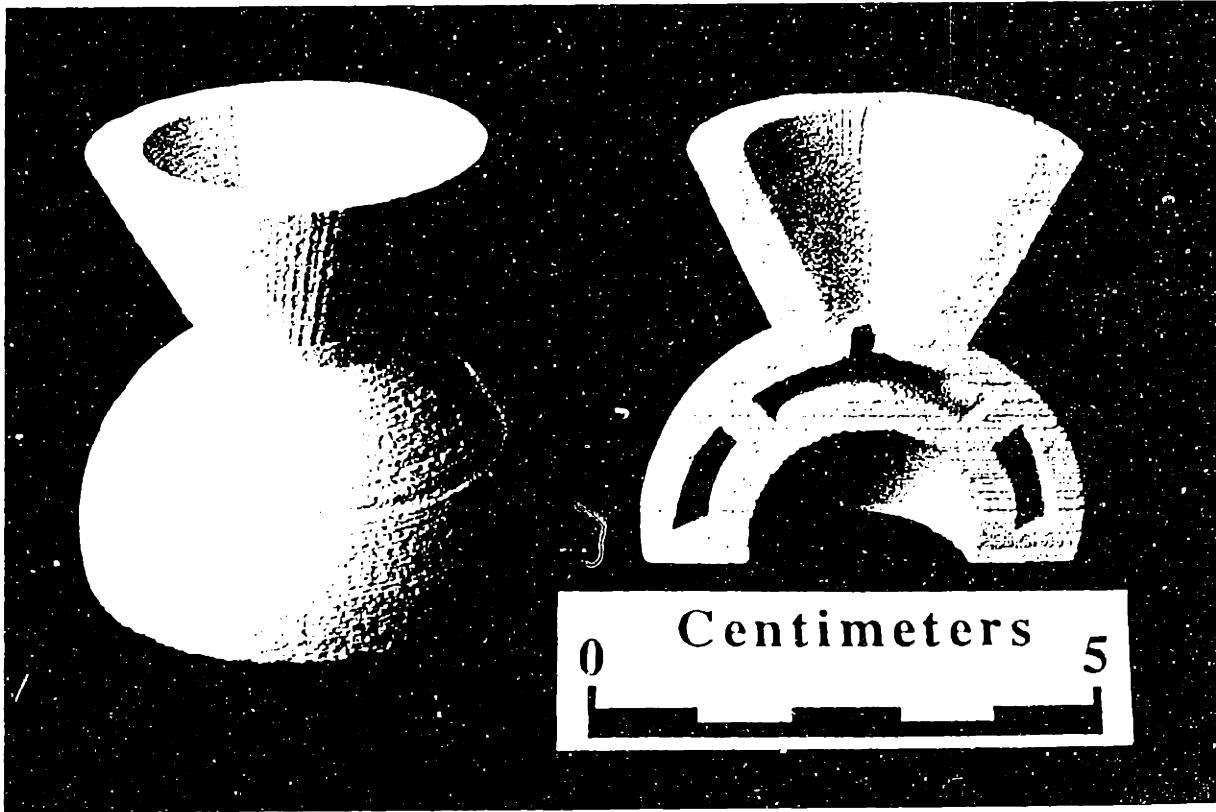


Figure 1.3: A part created using Three Dimensional Printing.

Three Dimensional Printing can be used to fabricate parts in a wide variety of materials, including ceramic, metal, metal-ceramic composite and polymeric materials. The objective of our work is to produce parts that will be used directly as prototype parts (both functional and aesthetic), and to produce parts that will be used directly as tooling.

### **1.3 Printhead Development**

This thesis documents the development of an electrostatically deflecting printhead for Three-Dimensional Printing. The concept of electrostatically modulating the flow of droplets from a continuous fluid jet is not new; a small number of companies have developed printheads that use this technique for high quality or high-speed ink-jet printing applications [Williams, pp 63-70].

Two such companies were initially contacted to see what was required to apply this existing technology to Three Dimensional Printing. Based on what was learned, it was decided to develop and build a prototype rather than modify existing ones. The primary reason was the existing designs' incompatibility with the binder, a colloidal silica suspension in water, which leaves a solid residue upon evaporating and has higher viscosity than water-based inks. A design with new techniques for binder handling and removing solids buildup was required.

Other difficulties were caused by the binder, which is printed through an alumina nozzle .0018" in diameter. This material tends to gel inside the conical nozzle tip, causing either a clogged nozzle, reduced flow, or a crooked stream. The resulting variability in the system exceeds that of typical commercial systems using water-based inks. Making the printhead robust to this variability required substantial development time.

A "next generation" machine will use up to one hundred nozzles in parallel to greatly increase the vertical build rate of printed parts. However, such a machine will not tolerate the variability present in the current system. For example, when starting to print a part on the current machine, a crooked stream is compensated for by pivoting the nozzle assembly, and the binder pressure is empirically tweaked to produce the correct flow rate. This process, which takes several minutes, would have to be repeated for each nozzle on a multiple-nozzle printhead. At this rate, setting up the machine could take longer than actually printing a typical part! These problems are addressed in chapter 5.

## **2. Continuous-jet Printing of Binder**

This chapter provides an overview of continuous-jet printhead operation. A more thorough description and analysis of associated phenomena is presented in Williams' masters thesis (1990).

### **2.1 Basic printhead layout and operation**

The printhead used in Three Dimensional Printing operates on the same principles as continuous ink-jet printing. Unlike drop-on demand printers, where droplets are forced out of a reservoir when required, continuous-jet printers produce a constant stream of liquid that either is printed or deflected into a droplet catcher.

In our application, electrostatic deflection is used to deflect charged droplets into a catcher for collection, and to allow uncharged droplets to pass undisturbed into the powder bed (figure 2.1). Selective printing is accomplished by charging certain droplets using a computer signal synchronized to the nozzle traverse.

This technique is used to selectively bind powder together in each cross-section of a 3-D printed part. The technology relies upon several principles which are discussed below.

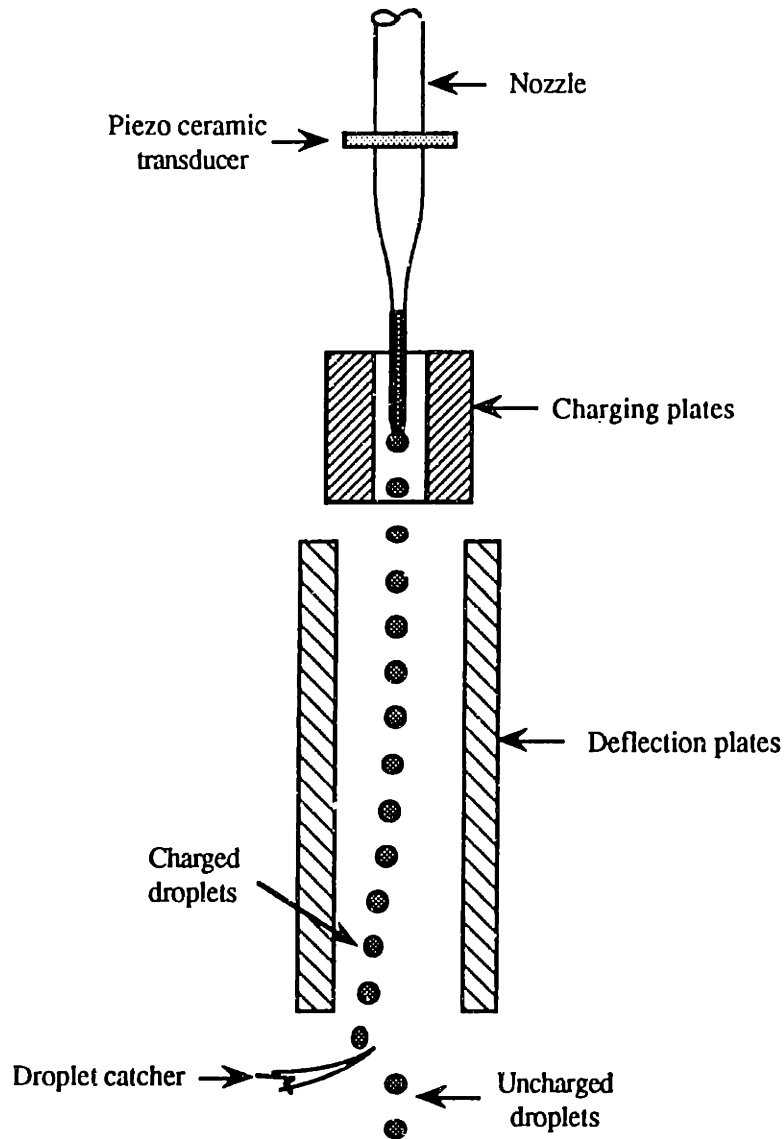


Figure 2.1: Schematic of continuous-jet printhead.

## 2.2 Formation of discrete droplets

Continuous-jet printers rely on the tendency of a fluid jet to break up into a train of droplets some distance away from the nozzle tip. Both the frequency of droplet formation and the distance from the nozzle tip at which individual droplets appear (breakoff length) can be predicted using formulae derived by Rayleigh [Williams, pp. 52-54].

Droplet formation is caused by infinitesimal disturbances in the stream which grow exponentially until spheres are formed. Since these disturbances are random in nature, the



resulting droplet train is irregular. However, a repeatable pattern of droplets can be produced by supplying a periodic disturbance near the nozzle tip. Piezoelectric transducers are ideal for this application because of their ability to induce vibrations at high frequencies. When a piezoelectric element is mounted on or inside the nozzle and excited at a frequency near the "Rayleigh" frequency, droplet formation can be synchronized to this frequency. These devices are discussed in detail in Appendix 1.

The formation of droplets may be accompanied by the appearance of "satellite droplets," which are approximately one-fifth the diameter of larger droplets. They typically will merge to adjacent droplets within a few wavelengths of their formation, but often interfere with printhead operation. These droplets can be eliminated under certain conditions by supplying enough piezo energy to prevent their formation. Satellite droplets are discussed in greater depth in Appendix 4.

## **2.2 Capacitive charging of droplets**

Capacitive droplet charging is a technique for controlling the path of individual droplets. The stream is aimed through a "charging cell," a conductive tunnel that can be raised to some potential relative to the stream. This tunnel can be a cylindrical hole or a pair of parallel plates. In either case, the stream effectively becomes one of the two conductors of a capacitor while the tunnel serves as the other (figure 2.2). The stream accumulates a charge proportional to the potential difference between the two.

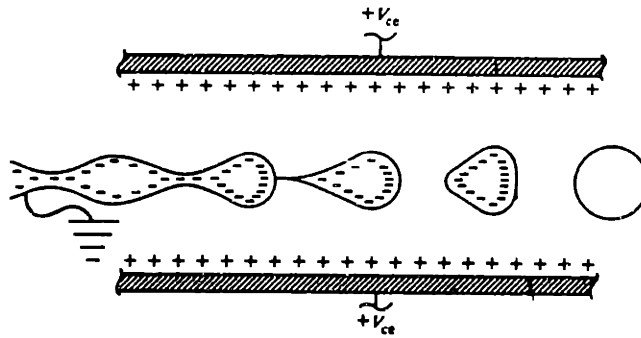


Figure 2.2: Droplet charging with parallel plates.

In order to place a charge on individual droplets, the charging tunnel is positioned so that droplet breakoff occurs near its center. This way, a newly detached droplet will carry the same charge density as the stream in its vicinity. Once a droplet has detached, its charge cannot be changed. The charge placed on each droplet is controlled by modulating the voltage to the charging tunnel. In order to control the path of individual droplets, the time constant of the charging process must be significantly less than the period of droplet generation. If this is not the case, some droplets will be partially charged and deflect less.

### 2.3 Droplet deflection

After passing through the charging cell, all droplets pass between a pair of parallel plates which establish an electric field transverse to the motion of the droplet. In this "deflection cell," droplets which were charged previously experience an acceleration due to electrostatic repulsion and are deflected into a droplet catcher which prevents them from reaching the powder bed. Uncharged droplets, on the other hand, are unaffected by the electric field and pass directly through to the powder. Typically, one plate is at some high positive or negative voltage and the other is at ground.

The trajectory of droplets can be changed by varying either the electric field or charge on the droplets. However, any change in electric field will affect all charged droplets inside the deflection cell at that time. In order to control droplets independently, their charges must be changed individually by modulating the signal to the charging cell rather than the deflection cell. Droplet acceleration can be predicted as a function of its mass, charge, and the deflection field. This is discussed at greater length in Appendix 2.

# 3. Printhead Design

## 3.1 Goals

This chapter describes the details of the printhead as of April 1991. This design is the result of lessons learned from several previous prototypes built over the previous months. Problems with clogging, shorting, poor visibility, and the lack of flexibility caused these devices to be extremely difficult to use. See Appendix 5 for a more thorough discussion of previous printhead designs and the evolution of the current design.

A list of criteria for an improved printhead, based on experiences from these previous attempts, is presented below. The prototype printhead was designed to satisfy this set of criteria. Bulletized items represent primary goals.

### Performance:

- Maximized mean time between failures
- Operation without manual intervention
- No shorting, sparking, clogging
- Crisp printing
- Clean, effective binder removal
- Accurate droplet placement (+/- .0005")
- Capable of deflecting individual droplets (must switch up to 30khz.)

### Convenience of use:

- Easy to clean
- Easy to operate; quick startup and shutdown
- Easy to see inside (facilitates strobe studies)

### Design:

- Easy to machine and assemble
- Easy to modify/upgrade
- Robust to noises:
  - binder flow rate
  - printhead traverse speed

- airflow across printhead
- crooked jet exiting nozzle
- variation in charging or deflection voltage
- Size/weight kept to a minimum
- Minimized distance from nozzle tip to part
- Supports proportional deflection
- As simple as possible

The goals of this printhead development were twofold: to assess the feasibility of using electrostatic deflection of binder for Three Dimensional Printing, and to get the machine up and running with a working printhead as soon as possible so the team could start making complex parts. These dual goals forced a tradeoff between an extended research effort and a more brute-force approach. However, every attempt was made to achieve an understanding of various observed phenomenon. This lowered the number of design modifications and ultimately shortened the development time.

Since printed parts at that time typically required up to six hours of print time, reliability and operation without intervention were of the utmost importance. Other factors, such as size, weight, produceability, and distance between nozzle tip and the powder bed, were secondary issues that were considered but not optimized.

At the onset of testing, the desired goal was loosely defined as a mean failure rate of once every ten hours. (A "failure" is any condition which impairs the operation of the Three Dimensional Printing machine in such a way that an acceptable part will not be produced.) However, it was recognized that this was a short-term goal and that greater reliability would ultimately be required. It was also accepted that a certain level of human intervention might be required, for example, pausing the machine every so often to clean printhead parts. While this relaxation currently does not pose much of a problem, it is not compatible with the long-term goal of a completely automated machine.

## 3.2 Overall design

The printhead in its current form is shown in exploded view in figure 3.1 and assembled in figure 3.2. Working drawings are shown in Appendix 6. The body is aluminum and bolts to a Thomson ball slide, which is in turn connected through a flexible coupling to a Normag linear motor. The key features of this design are discussed below.

•**Modularity.** The charging cell, high-voltage plate, ground plate / droplet catcher, and nozzle assembly are all easily removable. All of these except the droplet catcher can be removed without any tools, and electrical connections are automatically made when components are inserted. This allows components to be easily cleaned or inspected, and facilitates design modifications.

•**Visibility.** All deflected and undeflected droplets are visible from one side of the printhead. This allows the observation of several phenomena related to continuous-jet printing. Using a tele-microscope and a video camera, the behavior of individual droplets can be observed. This feature has led to a much greater understanding of the process.

•**Minimized clogging and shorting.** The design minimizes the occurrence of clogs and short-circuit conditions due to fluid collecting on components, and allows the printhead to recover quickly from such a condition with manual intervention. This was achieved by keeping the body and electrical connections far away from areas where fluid would tend to collect in the event that the printhead "floods."

•**Suitability for printing over long time intervals.** The design permits the printing of parts requiring several hours by eliminating sources of printhead failure, such as binder accumulation on components, and by minimizing maintenance during printing.

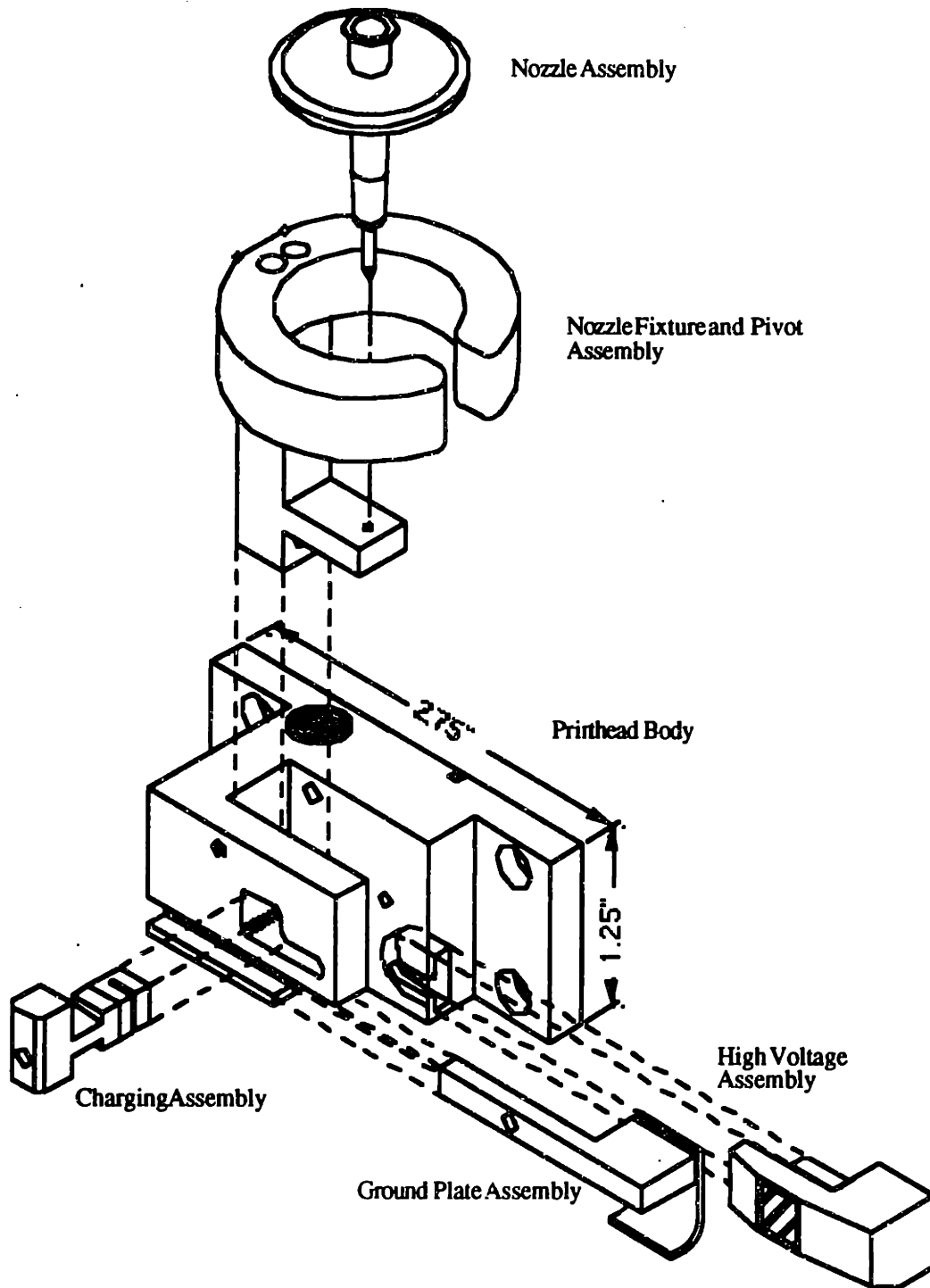


Figure 3.1: Exploded view of printhead.

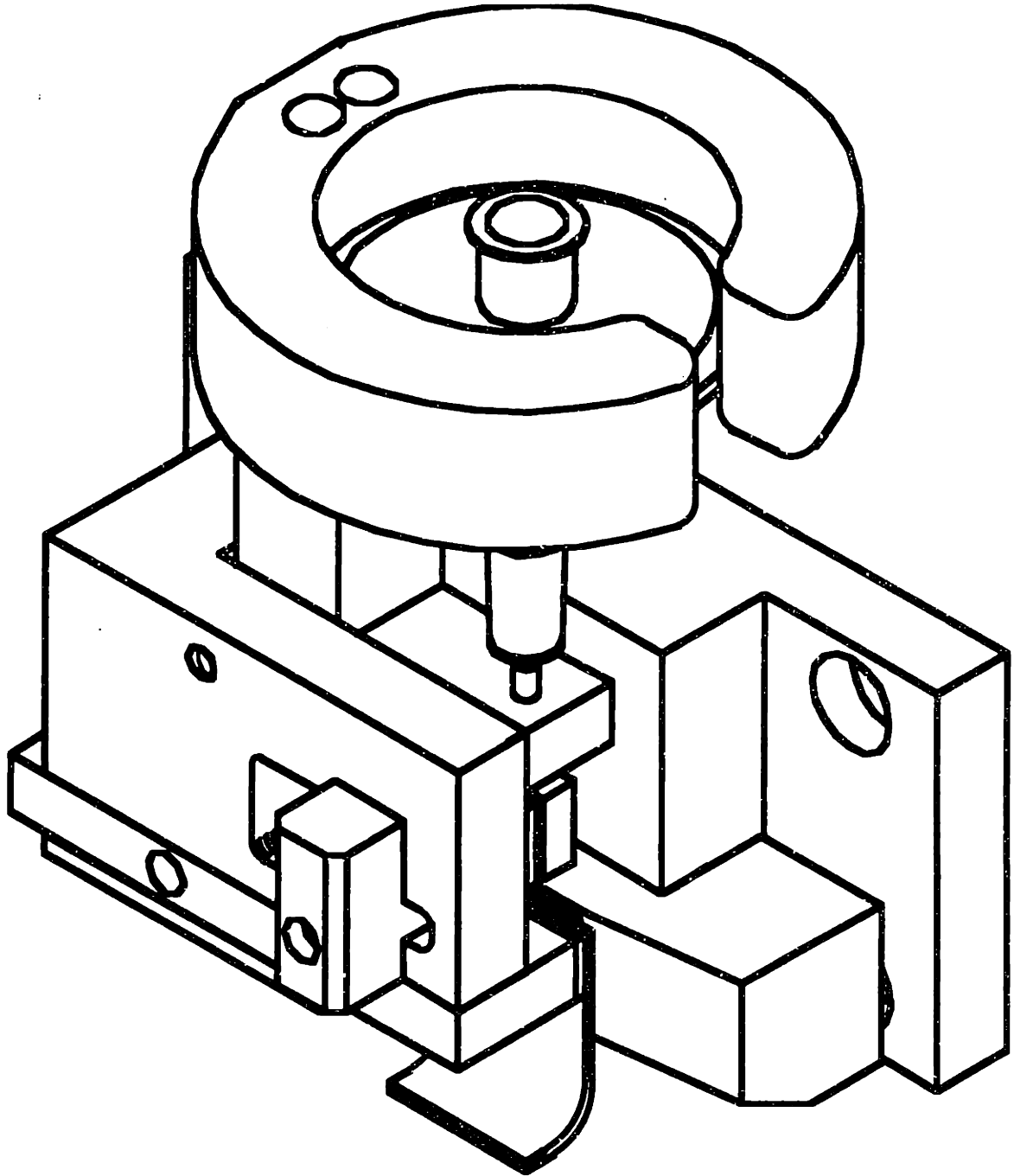


Figure 3.2: Assembled printhead.

Flooding typically occurs when the angle at which the jet leaves the nozzle (stream angle) causes droplets to collect on the walls of the charging cell. Since these walls are



closely spaced, fluid soon bridges the gap and collects there instead of shooting through. Once this failure is detected (visually or by an electronic current sensor), it is a simple matter of removing and cleaning the charging and deflection components.

### **3.3 Design details**

#### **3.3.1 Nozzle assembly and mounting components**

The nozzle assembly consists of the following components (see figure 3.3):

- 5 micron syringe filter (Gelman Sciences, Ann Arbor, MI)
- 26 gauge, 3/8" syringe needles (MIT lab supplies)
- .188" O.D. x .040" I.D. x .020" thick piezoceramic disk (Piezo Kinetics, Inc., Bellafonte, PA)
- Wire-wrap wire leads to piezo and to syringe needle
- Wire-bonding nozzle, .0018" Dia., P.N. 1572-18-375P (Gaiser Tool Co., Ventura, CA)
- Aluminum and teflon mounting bracket and pivot arm.

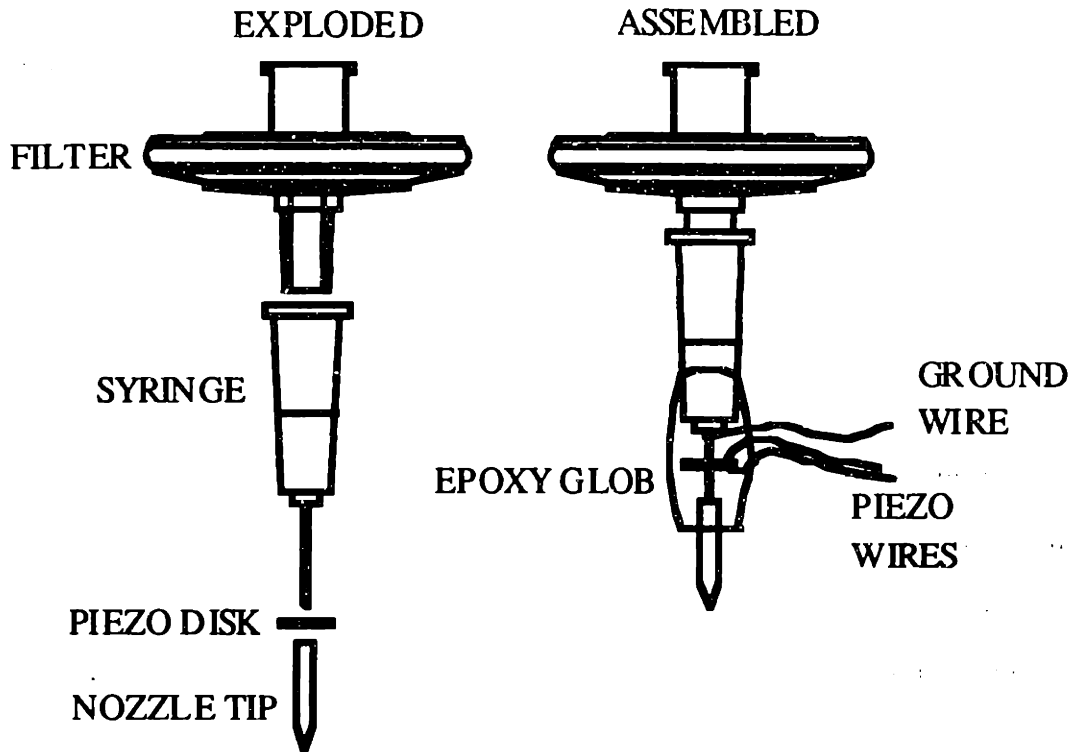


Figure 3.3: Nozzle assembly components.

Working in a laminar flow hood, the syringe needle is mounted to the syringe filter, a wire is wound around the needle if a non-conducting nozzle is to be used, and the piezo and nozzle are slipped over the needle. The assembly is placed in a jig and epoxy is applied to make a seal and fix components in place.

The completed nozzle drops into the mounting bracket, which pivots on a dowel pin inside the printhead body. This allows the nozzle to compensate for errors in stream angle, so the stream can be centered between the charging plates. Construction in the jig places the nozzle's exact tip very close to the center of rotation.

### 3.3.2 Piezo excitation

The piezo disk transfers its energy to the nozzle tip through the epoxy it is encased in. It is energized using a function generator (Leader model LFG-1300S) connected to an amplifier (Krohn-Hite model 7500). Generally a sine wave signal at up to 200 volts peak-

to peak, in the range of 40 to 65 kilohertz, is applied to the piezo. This results in a breakoff distance of around .090", which places it close to the vertical center of the charging plates.

### **3.3.3 Droplet charging assembly**

The charging assembly consists of an aluminum part with a .025" wide slot connected to a teflon handle and fixture (figure 3.1). This slot effectively creates a set of charging plates. These charge plates receive a signal which is either at ground or at some fixed potential between 24 and 120 volts. The expected charge/mass ratio with this design is discussed in Appendix 2.

The slot design allows the charging assembly to be removed or installed without disturbing the binder stream. This way, the stream can be centered before the plates are in place, thereby preventing charging cell flooding. This eliminates a common cause of startup failure with previous prototypes.

### **3.3.4 Deflection cell**

The deflection cell is the printhead region where charged droplets enter an electric field and are deflected towards a catcher which prevents them from being printed into the part. The cell consists of a high-voltage plate, which is typically charged to a potential of -1000 to -3000 volts, and a plate which is at earth potential (see figure 3.4). The spacing between this plates is approximately .05", which creates an electric field as high as minus  $2 \times 10^6$  volts/meter. (Air breaks down at  $3 \times 10^6$  volts/meter). The deflection voltage is varied during startup to accelerate charged droplets in a trajectory which causes them to land in the proper location on the catcher. Predicted droplet accelerations for this design and the choice of plate spacing is discussed in Appendix 2.

The high-voltage plate assembly is a thin stainless steel plate cast into an epoxy block which is shaped to slide in and out of the printhead body. An electrical contact is automatically made when the plate is slid into position.

### **3.3.5 Droplet catching and removal**

Two successful droplet catching and removal arrangements were built. The first, shown in figure 3.4a, is a stainless steel plate which curves away at the bottom. This part serves a dual function as both a ground plate and a droplet catcher. Deflected droplets strike the plate at a shallow angle, follow the plate's curve, and collect underneath. When the printhead is stationary, binder drips from the plate into a collection trough. When the printhead is moving, drops are flung off the plate as the printhead accelerates at the end of each traverse. These drops collect in troughs at either end of printhead travel and travel down tubes to collection bottles. Binder which collects in these bottles can then be recycled.

The second configuration, which is currently being used on the machine, is shown in figure 3.4b. Here, the ground plate and droplet catcher are two separate components. Deflected droplets curve past the ground plate and strike the catcher directly. They collect there until gravity or inertial forces cause a drop of binder to fall into the collection trough. While this design functions basically the same way, it has the advantage of a ground plate which never becomes wet with binder. This minimizes the chance of buildup occurring in the deflection cell. The drawback of this design is that it is less compact and has more parts.

### **3.3.6 Drive electronics**

Computer control of the printhead during a typical part requires rapidly switching a signal between ground and up to 120 volts. This was accomplished using the circuit shown in figure 3.5. The computer supplies a TTL signal which is high for printed (undeflected) droplets and low for unprinted (deflected) droplets. This signal is the input to the circuit box. The TTL signal is transmitted by an opto-isolator with Schmidt-trigger outputs. This device protects the computer from high voltage and minimizes the effects of

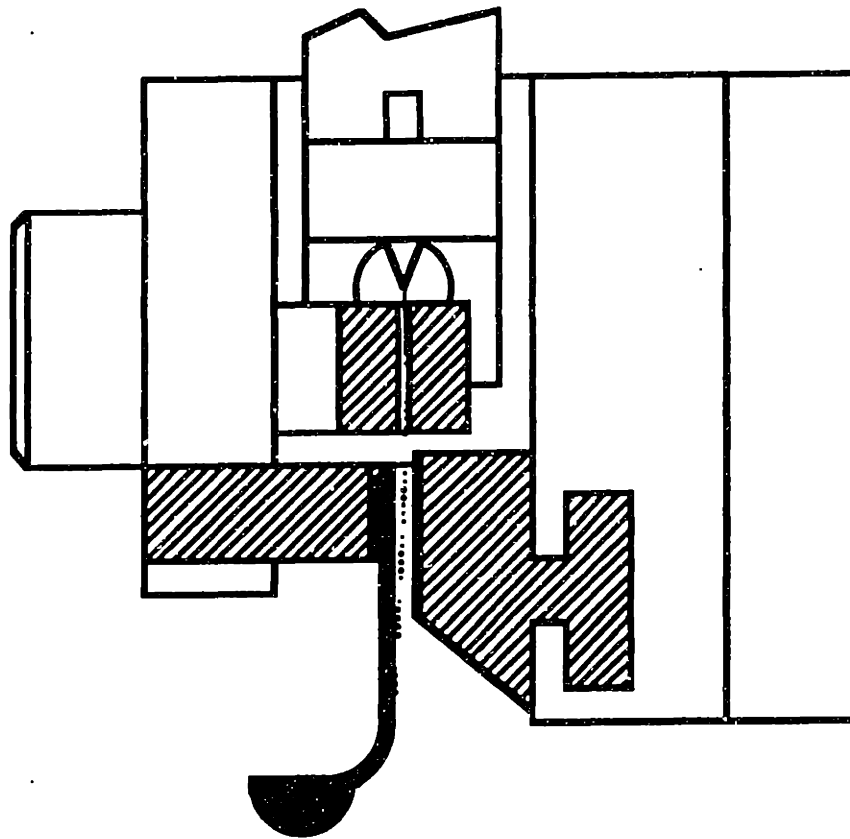


Figure 3.4a: Catcher configuration with combined ground plate/catcher.

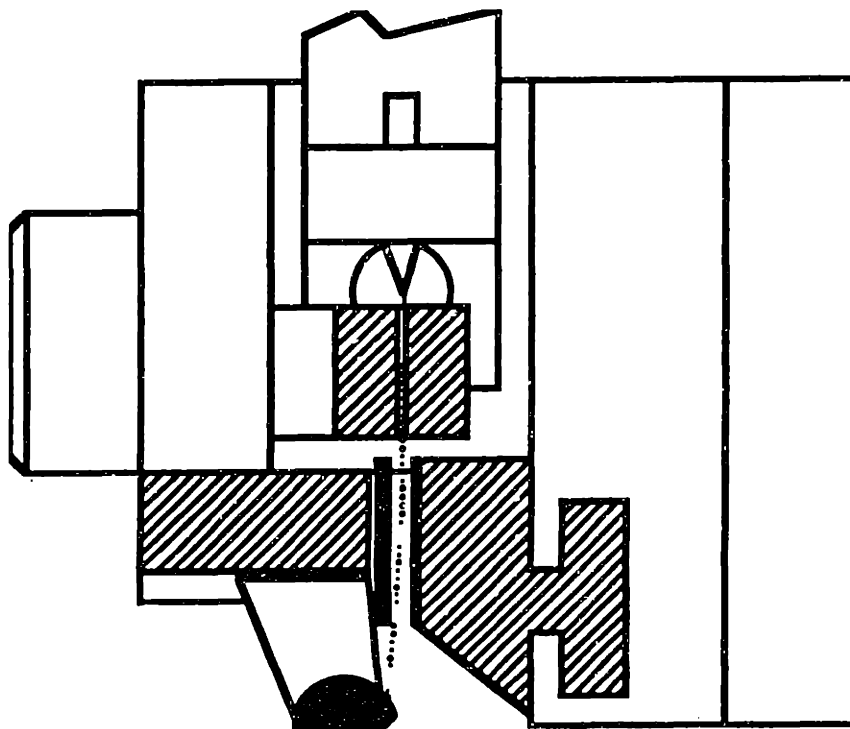


Figure 3.4b: Catcher configuration with independent catcher.

line noise. This output is fed to the base of a switching transistor with the supply voltage (120 volts) on its collector. The output is measured between the collector and ground.

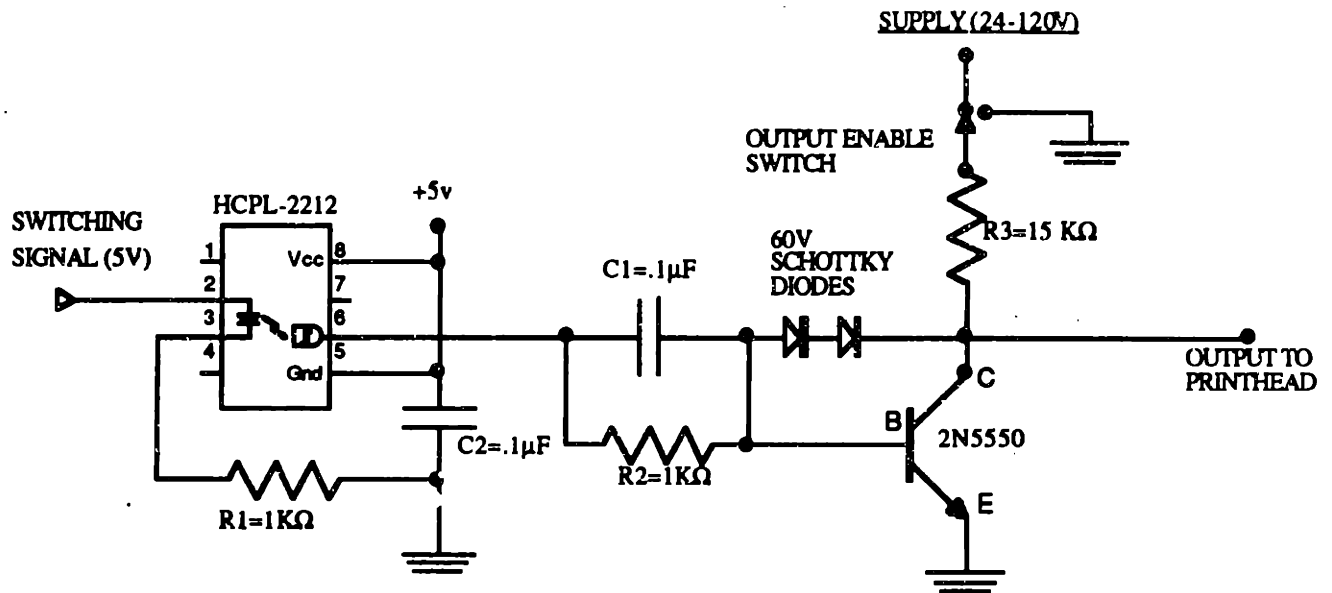


Figure 3.5: Drive electronics for electrostatic switching.

When the signal goes high, the transistor switches on and the collector voltage drops to zero. This causes the charging plates to see a ground potential, and droplets are undeflected. When the signal goes low, the transistor shuts off and there is no current between the collector and emitter. Since there is also no current through resistor R3, the output is at the supply voltage, and droplets passing through the charging plates become charged.

The Schottky diodes and capacitor C1 were required to improve the switching characteristics in order to produce an acceptable signal at the required voltages and frequencies (discussed in greater detail in Appendix 3). The diodes prevent transistor saturation by reducing the base current when the transistor nears saturation, reducing the delay time in transistor shut-off. Capacitor C1 is a "speedup" capacitor which increases

base drive current during turn-on transitions, and provides a current pulse to remove base charge at turnoff, resulting in faster rise and fall times [Horowitz, Hill p 908].

### **3.4 Discussion**

The greatest challenge in this design task was to develop a printhead that was robust to the noises associated with the nozzle and the binder. Crooked streams, which could mean deviations in any direction of up to 20 degrees, forced the abandonment of a charging cylinder and required conservative spacing between charging and deflection plates, the inclusion of a nozzle pivot and a mechanism for easily removing the charging plates. Nozzles that produced straighter streams would permit a much simpler and more efficient printhead. Closer charging plate spacings would require less voltage, leading to several positive benefits including faster switching time, simpler electronics, and cheaper power supplies. A more efficient printhead would require a smaller charge on each droplet for full deflection, resulting in reduced electrostatic interactions between charged droplets.

The colloidal silica binder has created a host of problems including clogged nozzles and crooked streams. This was alleviated through the addition of a binder/water switch just upstream of the nozzle and establishing the practice of running water through nozzles before and after printing parts.

Solidified binder caused printhead components to bind in place and forced a strong emphasis on preventing flooding. With the combined ground plate/catcher configuration of figure 3.4a, binder tends to dry up and eventually either build up or flake off the ground plate in the vicinity of the spot where the stream hits the plate. This solid binder could potentially interfere with the deflection field or the stream. These binder characteristics forced conservative spacing between the high voltage and ground plates.

Throughout the design and testing process, an emphasis was placed on understanding and solving problems rather than eluding them. For example, a previous catcher design

was collecting buildup on a knife-edge for no apparent reason. It was recognized that the printhead could be made to work in spite of this by adding a stationary "scraper" that would remove this buildup with each pass of the printhead. Instead of implementing this, however, a microscope was used to identify the source of the buildup as partially charged droplets (artifacts of the electronic circuitry). As a result, the electronics were improved, and new catcher design with no knife-edge was tested and implemented. This eliminated the need for a scraper and resulted in a simpler, more elegant design.



## **4. Performance of Prototype**

As of late February, 1991, the printhead was operating successfully for the construction of parts requiring up to twelve hours of print time. During some runs, intervention was required every few hours to remove buildup caused by satellite droplets collecting on the ground plate, or buildup on the high-voltage plate caused by airborne binder. On other runs, the printhead ran with no intervention. Overall, its performance is satisfactory at this point. Given the progression from a prototype that had to be coaxed into working for a few minutes at a time to a device which runs unattended for hours, this has personally been extremely rewarding. However, the printhead is by no means optimized and there are several issues related to accuracy, reliability, and practicality that warrant further discussion.

### **4.1 Effects of satellite droplets**

Satellite droplets are created when the binder stream first breaks up into droplets under piezo excitation. Their occurrence can be minimized but they are difficult to prevent. These droplets are deflected more than the larger droplets, because they receive the same charge but have less mass. Figure 3.6 shows a "stalagmite" created by satellite droplets collecting on top of each other near the top of the ground plate. This eventually causes printhead failure as this stalagmite continues to grow until it interferes with the stream. Currently, their formation is minimized by empirically choosing a piezo frequency that causes the slowest buildup. Satellites are discussed at length in Appendix 4.

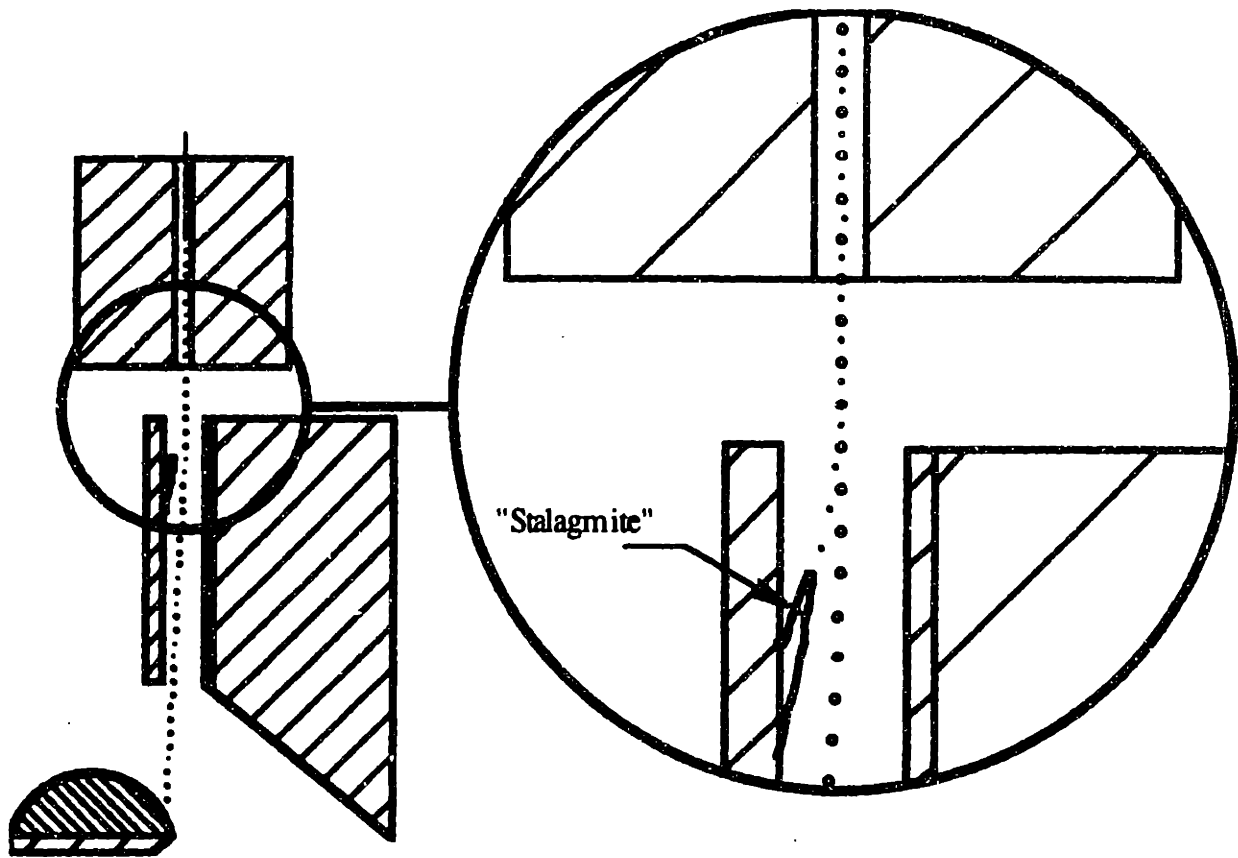


Figure 4.1: Buildup due to satellite droplets (worst case).

## 4.2 Buildup on printhead components

Even when satellite droplets do not seem to be forming, binder slowly accumulates on the edge of the droplet catcher, requiring that the printhead be inspected and this buildup be removed every two hours or so. It is possible that this problem is caused by partially charged droplets, a result of a droplet breakoff occurring while the charging signal has not risen fully (see Appendix 3).

## 4.3 Droplet placement error

Printhead performance can be measured by the accuracy of droplet placement in the powder bed in the direction of travel and the transverse direction. Placement error in the

direction of travel results from aerodynamic noise and delays in the electronic hardware, while sources of error in the transverse direction include aerodynamic noise, play in the Thomson linear bearing, and unwanted charge on "uncharged" droplets. In general, placement error does not appear significant compared to other parameters affecting overall part dimensions, specifically the powder-binder interaction. However, individual droplets at the beginning of each line segment are generally very misplaced. This results from several known phenomena which are discussed below.

#### **Aerodynamic drag**

In any droplet train, aerodynamic forces will be greatest on the first droplet, which creates a slip stream for the droplets behind it. This will cause the leading droplet to decelerate more than trailing droplets, causing it to strike the powder later than it should.

#### **Partial droplet charging**

Ideally, the charging cell is driven by a square signal. However, due to limitations in the speed of the electronic circuitry, voltage transitions require several microseconds. Droplets which form during these transitions will receive an incorrect charge, and will be deflected incorrectly. See Appendix 3 for a more detailed explanation.

#### **Merged droplets**

The first droplet of any undeflected droplet train was observed to be slightly misplaced and somewhat larger than the droplets trailing it. Closer observation using a strobe and a square wave charging signal revealed that this droplet is actually the union of the trailing charged drop and the leading uncharged drop of two adjacent droplet trains (figure 4.2). Electrostatic repulsion among the charged drops displaces the trailing charged droplet far enough to come in contact with the leading uncharged droplet, which is normally one full wavelength away. The two merge to form one larger droplet with a normal charge. Since it only has half the nominal charge to mass ratio, it is only partially deflected.

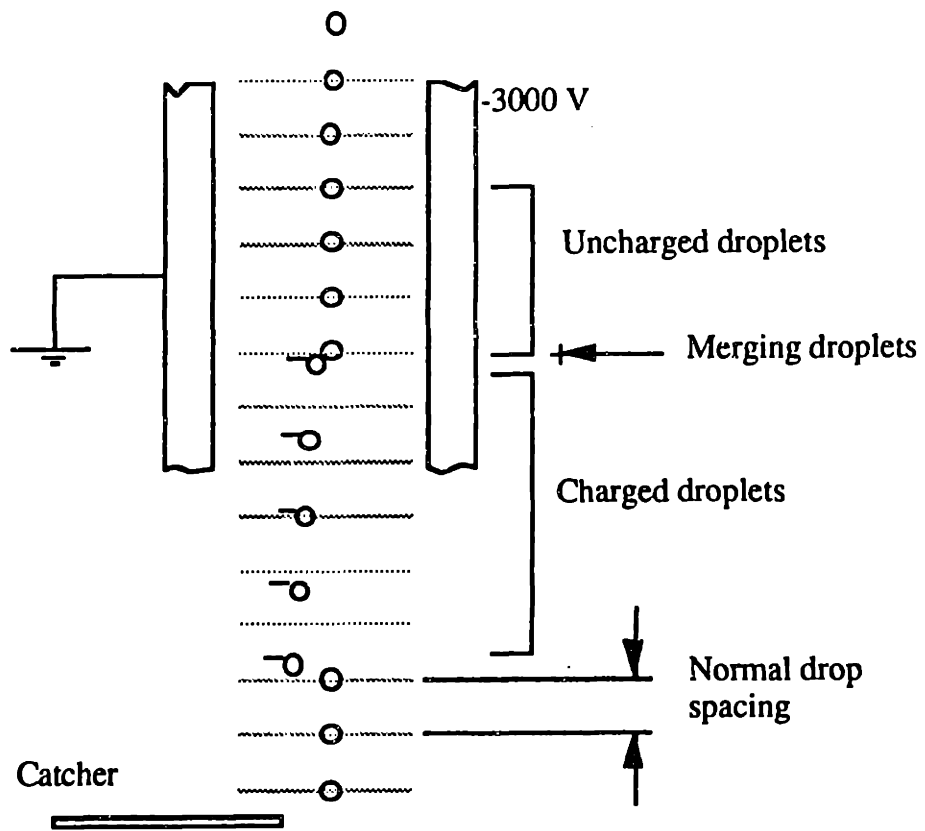


Figure 4.2: Observed merging of charged and uncharged droplets.

In order to print very short line segments, the printhead must have the ability to produce accurate droplet trains containing very few droplets. For reasons discussed above, several of the leading droplets of any droplet train will be misplaced. The effects of these errors have not been studied, but they may result in poor surface finish. For very short pulses, the number of misplaced droplets will be on the same order as the number of correctly placed droplets. This limits the minimum feature size.

## **4.4 Set-up time, startup/shutdown**

There are three major components of set-up:

**Producing an acceptable flow rate.**

This is done by tweaking the pressure in the binder tank and taking readings until the desired flow rate is obtained. This task will ultimately be automated using a closed loop pressure regulator.

**Compensating for a crooked stream.**

This can be done either by pivoting or rotating the nozzle in its housing.

**Minimizing satellites.**

This step is often the most time consuming. Different frequencies are tried until the rate of satellite buildup appears to be minimized. A difference of 1KHz. can mean the difference between cleaning the printhead once every hour or once every minute.

In order to reach the ultimate goal of a machine which starts up automatically and prints a part without intervention, more reliable nozzles are needed and the satellite problem must be eliminated.

## **4.5 Suggested improvements**

Goals for improvement include improving reliability, minimizing intervention, reducing set-up time, and improving resolution and accuracy. The current wire-bonding nozzles cause uncertainty in stream angle and flow rate which in turn affect reliability and set-up time. Therefore, orifice plates with electroformed holes are being investigated to replace the current nozzles (see chapter 5).

Improved resolution requires speeding up the switching electronics, which should be achievable with further research. Improved accuracy will result from using a more

accurate slide, improved electronics, and a reduced charging voltage to minimize interaction between droplets.

The implementation of reliable nozzles would have significant effects upon printhead performance. If stream error never exceeded one degree, given the current plate dimensions, the stream could never strike the charging plate. The pivot assembly would therefore no longer be necessary, reducing weight and size. The charging plates could be placed closer together, requiring less charging voltage for a given charge/droplet, which in turn would make the electronics simpler and faster. If breakoff occurred closer to the nozzle tip than it currently does, the charging plates could be shortened. The deflection cell could also be made more efficient and shortened. This would result in a smaller and lighter printhead, and accuracy would improve since the nozzle tip could be brought closer to the powder bed.

The difficulty in eliminating satellite droplets has been the major impediment to improving reliability. Appendix 4 suggests enough possibilities to warrant extensive experimentation on this subject; it is likely that some subset of these experiments will be performed in the future. To date, one easily implemented experiment has been performed.

Satellites result, at least in part, from insufficient piezo energy being delivered to the stream, which suggests either increasing energy input or improving the efficiency of the configuration. Since we are operating at the limits of our equipment, the latter approach must be taken.

Two proposed solutions are currently being tested. First, since all energy must be transferred to the stream through the epoxy encasing the piezo disk, nozzles are now assembled using an alumina-impregnated epoxy to reduce compliance and losses. Secondly, nozzles are currently being assembled with two disks wired either in series or parallel.

Figure 4.2 compares the performance of three configurations using alumina-impregnated epoxy. Satellite droplets seem to be minimized at frequencies that produce the shortest breakoff length, which is easily measured using a strobe and microscope. This graph was created for a particular nozzle/piezo assembly by changing the wiring for each set of data points. This rather bizarre response is a "fingerprint" for the assembly; each particular one has different sets of mechanical resonances which cause the shortest breakoff lengths at a given flowrate. The shortest breakoff length is obtained by driving one piezo at 50 KHz.; however, any slight deviation in frequency will cause a sharp change in the response. Driving two piezos in parallel produces a response which is most robust to changes in frequency or flowrate.

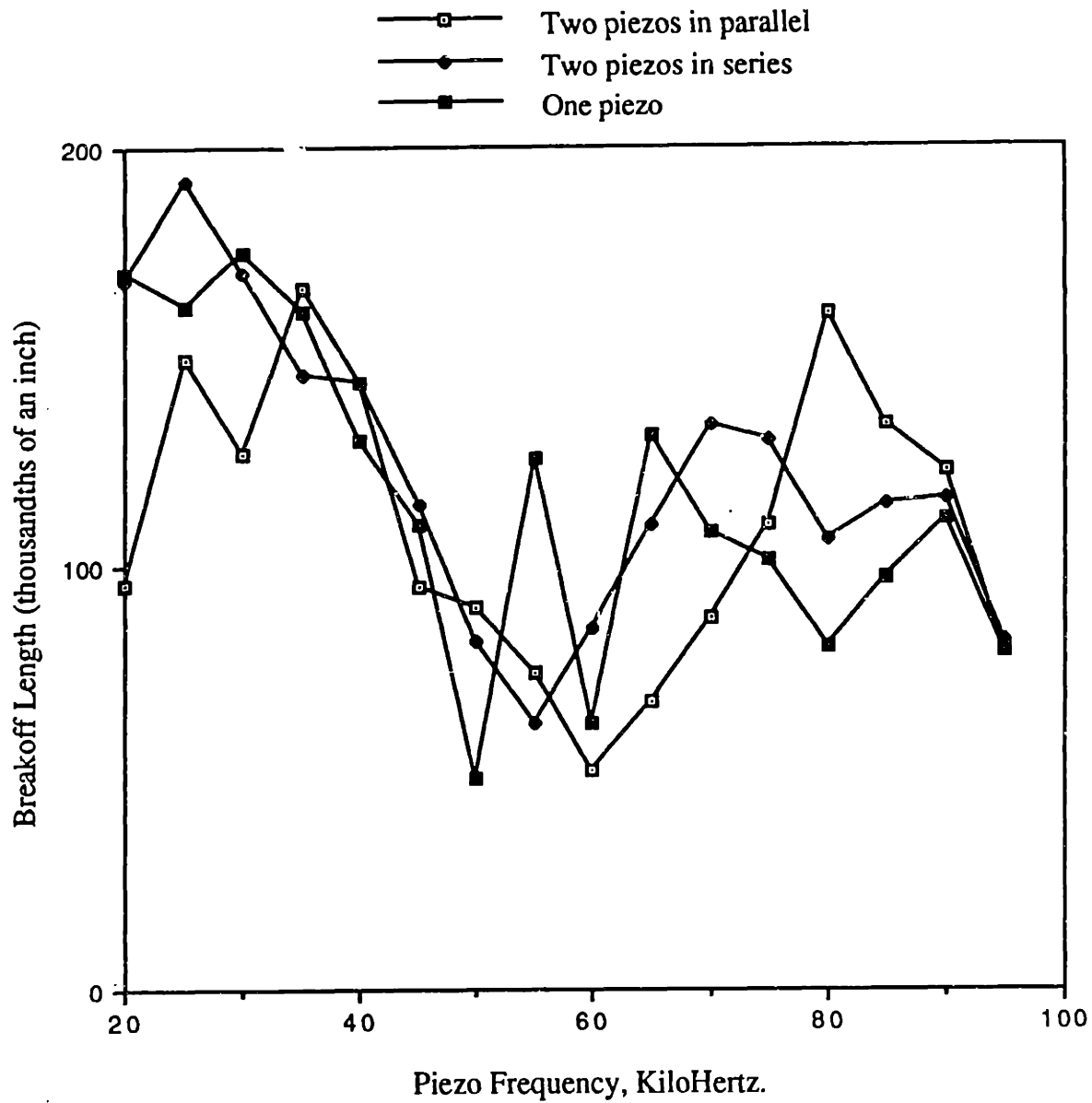


Figure 4.3: Breakoff length vs. stimulation frequency for several piezo configurations.



# 5 Towards a Multiple-Nozzle Printhead

## 5.1 Requirements

The ability to print parts using many nozzles in parallel will be crucial to the commercial viability of Three Dimensional Printing. A new 100 nozzle machine is currently being designed that will be capable of building a 2' x 1' x 1' part in under 12 hours. The streams will be spaced one tenth of an inch apart, resulting in a ten inch long printhead assembly. This will require 100 identical printhead cells, each one tenth of an inch across. The cells will function basically the same way as the current printhead, however, the following issues must be addressed before this technology can succeed.

The nozzles must produce straighter jets.

The 1/10" envelope will require much tighter charging and deflection plate spacings than on the current printhead, and devices to compensate for crooked jets are undesirable. Additionally, inaccurate printing will occur if adjacent streams do not strike the powder the same distance apart. Assuming a distance of 1/2 inch from nozzle to powder and a desired accuracy of  $\pm 0.001$ " in the direction transverse to printhead motion, the allowable stream error would be

$$\pm \arctan \frac{.001}{.5} = \pm .11^\circ = \pm 2 \text{ milliradians.}$$

Since it is not clear that error can be kept this small, stream errors in both the transverse and high-speed axes will be measured using line array cameras and compensated in the software. Fast-axis errors will be compensated using a time delay, while transverse errors will be compensated using proportional deflection. In the latter case, error correction will be limited to about  $\pm 0.10$ ," so the maximum allowable error will be

$$\pm \arctan \frac{.01}{.5} = \pm 1.15^\circ .$$

The nozzles must be far more reliable.

Given the number of nozzles, their failure rate must be substantially decreased. The nozzles should produce consistent flow rates since pressure will be the same for all nozzles.

A single "nozzle block" is desired.

For fabrication and assembly reasons, a single plate with a set of nozzle orifices built into a pressurized body is superior to a set of individual nozzle assemblies. The current configuration could not be squeezed into the desired spacing.

A new piezo configuration will be required.

A different excitation technique will be required since the nozzle geometry will be completely different. Some possible configurations are discussed later in this chapter. It should produce consistent droplet breakoff lengths for all nozzles (.020" to .050") and minimize satellite droplet formation.

To address these requirements, current research is investigating the use of thin plates with multiple orifices, rather than conical nozzles, in conjunction with some form of piezo stimulation. This configuration, which is used by related industries, is promising because the orifice geometry is less prone to interference from internal buildup and could potentially be manufactured more accurately than the current wire-bonding tools, resulting in greater reliability, accuracy and uniformity in the stream.

## **5.2 Orifice plate configurations and experiments**

### **5.2.1 Sources**

Thin plates with .0018" (46 micron) holes are available from a number of vendors. They use several techniques which are summarized below for selected vendors.

<b>Process</b>	<b>Vendors</b>	<b>Quoted tolerance</b>	<b>Materials</b>
Laser drilling	Precision Laser Services (IN)	$\pm.0001''$	Stainless steel
Etching	Towne Labs (NJ)	$\pm.0003$ $\pm.0002$	Stainless steel Ni, Cu bimetal
Electroforming	Buckbee Mears (MN) Veco Perforated Products (MA)	$\pm.0001$ $\pm.0002$	Nickel, gold Nickel
Punching/pre- cision drilling	Ladd Research Industries (VT)	$\pm.00005$	Platinum, molybdenum

Stock items were obtained from some of the above companies for experimentation. Some vendors produce aperture plates for use in electron microscope; others use artwork masks to produce a complex shape. Disks were obtained since they were more readily available. At this stage, laser drilled holes have been investigated and electroformed holes are being investigated. Thorough research into other possibilities has not yet been performed.

### **5.2.2 Laser-drilled orifices**

.0018" holes in .005" thick disks with a .250" O.D. were tested in a fixture which allowed pressure to be built up in a small reservoir of filtered fluid on one side of the disk.

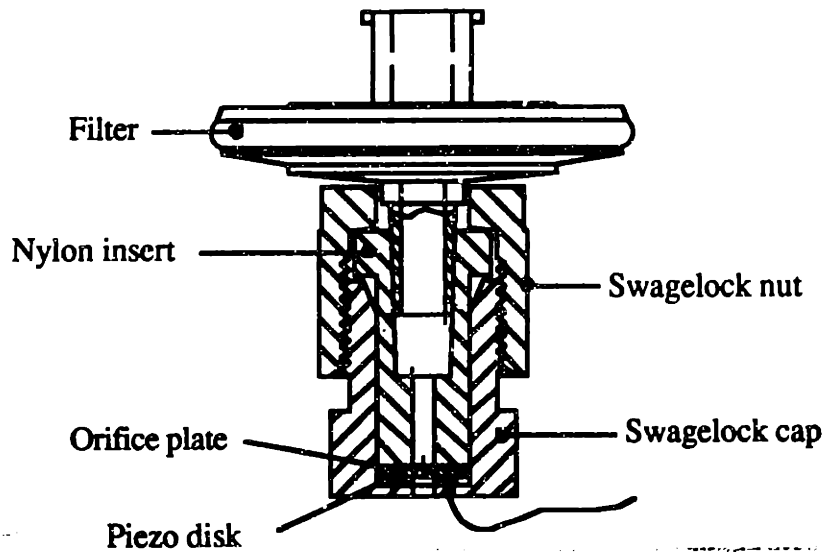


Figure 5.1: Fixture for testing orifice plate

Clogs occurred frequently, but light could still be seen through "clogged" plates after their removal, suggesting that the orifice was obstructed by a large particle which was held against it by pressure upstream. Since the components are assembled in a dirty environment, it is easy for particles to enter the fixture prior to assembly.

Straight streams were never observed using these plates. Under the microscope, the hole appears very irregular and jagged (see figure 5.2). Laser-drilled holes have therefore been ruled out as a possibility.



Figure 5.2: A laser-drilled hole in a .005" thick stainless steel plate..

### 5.2.3 Electroformed orifices

To create electroformed holes, nickel is plated over a photoresist dot to create the cross section shown below.



Figure 5.3: Cross-section of an electroformed hole used as a nozzle.

Material can flow either way through this hole. The optimum direction will depend on the binder interaction with the plate (binder sometimes gels on internal surfaces) and the stream characteristics for a rounded or a sharp-edged orifice.

Binder was successfully printed through a .0018" electroformed hole but no straightness error measurements have been made to date. Disks .001" thick and .1" in diameter will be tested for straightness and reliability. The holes in these plates appear very regular and smooth.

## **5.3 Possible piezo configurations**

Future research will investigate efficient piezo stimulation of a multiple nozzle system.

This can be handled several ways, as outlined below:

One transducer can be used to stimulate each nozzle.

Since a linear array of orifices in a single plate is likely to be used, each piezo would be bonded directly to the orifice plate in the vicinity of each nozzle. Alternatively, orifices could potentially be constructed from piezoelectric material, with electrodes patterned onto the material.

One transducer can be used to stimulate all nozzles.

An example is the Diconix model 2800 high-speed printer, which has 1600 jets in two rows along a 13 inch long orifice plate. One end of the plate is vibrated using a piezo, and vibrations travel along the plate. Because of the travelling wave, it is difficult to synchronize droplet formation.

Several transducers can be used to stimulate sets of nozzles.

This alternative might permit "plane wave" excitation, which is achievable with shorter orifice plates. In this case, all orifices would receive a signal with the same phase, which allows synchronous droplet formation. A piezo might be mounted along the entire length of each assembly, or could supply its energy at one point of the assembly. The orifice assembly might be tuned to resonate at the piezo driving frequency.

### **5.3.1 Mechanisms for causing droplet formation**

The piezo supplies periodic disturbances to the stream which cause droplet formation. However, it is unclear whether these disturbances are transmitted by pressure waves within the fluid, or by direct vibration of the orifice. The nozzle assembly shown in figure 3.3 could potentially function by either mechanism: energy could be transferred through the epoxy to the syringe, where vibrations would set up a pressure wave in the fluid.

Alternatively, energy could be transferred to the nozzle, causing vibrations at the tip. Perhaps there is a combination of effects. The pressure-wave effect was tested using the setup in figure 5.3. A piezo is suspended in the fluid, requiring that all its energy be transmitted through the fluid. This device created uniform droplets with a .080" breakoff length at 1.5 cc/minute. This is comparable with the performance of the configuration currently in use.

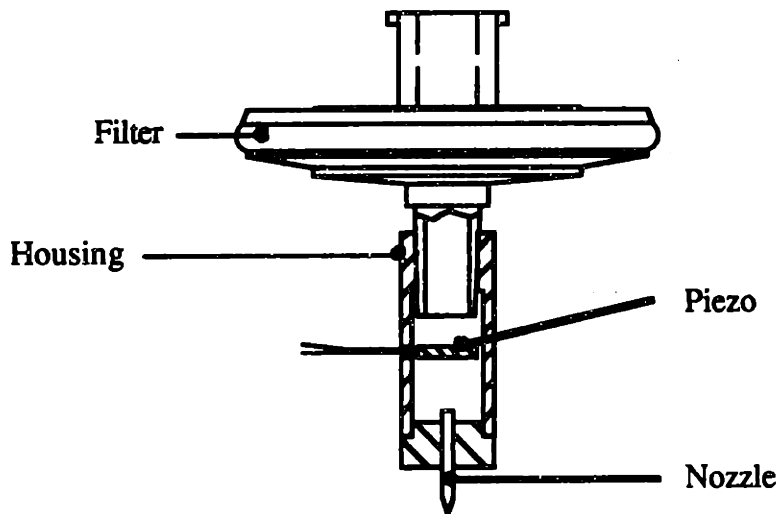


Figure 5.4: Device to test pressure-wave stimulation of fluid jet.

Efficiency of piezo stimulation can be optimized by taking advantage of mechanical resonances in the orifice mounting block. The configuration shown in figure 5.4 provides an example. This device consists of three piezo transducers, a solid metal block with a narrow flow cavity, and a thin orifice plate epoxied on to the resonator body. Two of the piezos supply energy; the third is used as a pickup to measure the amplitude of vibration.

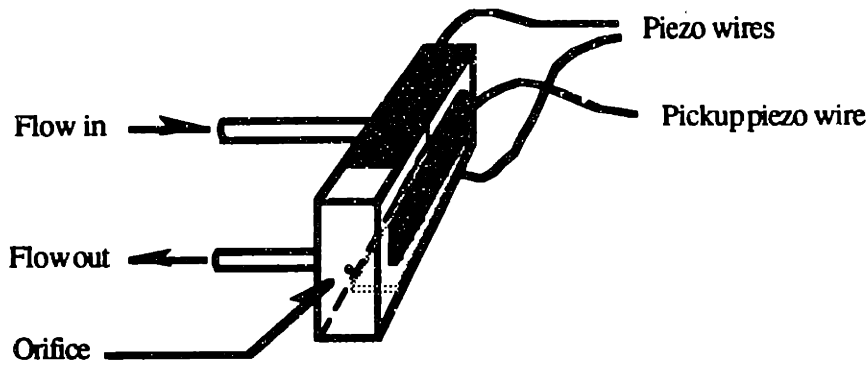


Figure 5.5: A resonator assembly.

This device will only produce reliable droplet breakoff when piezos are energized with a signal within a few hundred kiloHertz of the body's resonant frequency. However, it is far more efficient than the piezo disks we are currently using, producing droplet breakoff 20 mils from the orifice with a 5 volt sine wave (as compared to 90-120 mils using over a 100 volt sine wave).

## 5.4 Steps to Prevent Clogging

Due to the increasing complexity of assembling orifice plate fixtures, and the impracticality of using sterile components, it is becoming more difficult to prevent foreign material from entering regions inside the assembly that could cause clogging. There are at least two steps that can be taken to alleviate this problem:

Keep all components super-clean prior to and during assembly.

Machined parts, for example, could be placed in a filtering bath and/or ultrasonicated to remove particles, and kept inside a laminar flow hood throughout the assembly process.

Implement cross-flushing to remove particles in the assembled system.

Instead of pumping all binder through the orifice nozzles, the majority of the binder would be recirculated back to a storage tank for refiltering. This way, if particles were introduced during assembly, it is likely that they would be flushed out instead of causing a clog. Two possible configurations are shown below. Each system contains a large binder



storage tank, a peristaltic pump (constant flow) leading to a smaller reservoir, filter units, and a printhead assembly with a return line for recirculating binder.

In figure 5.5a, a pressure source is used to push fluid through the filters and the printhead. Fluid exits through a side passage into a small reservoir with a free surface (this guarantees that exiting fluid does not affect pressure inside the printhead). Another peristaltic pump then pulls this fluid back into the reservoir.

In figure 5.5b, a peristaltic pump drives fluid through the filter, and accumulator, and the printhead. Recirculating fluid returns directly to the reservoir, through a resistive tube. The advantage of this configuration is that it requires only two pumps, one of which does very little work refilling the reservoir, and is a low pressure system. Its disadvantage is that the action of a peristaltic pump may not be smooth, and it may be more difficult to regulate printhead pressure.

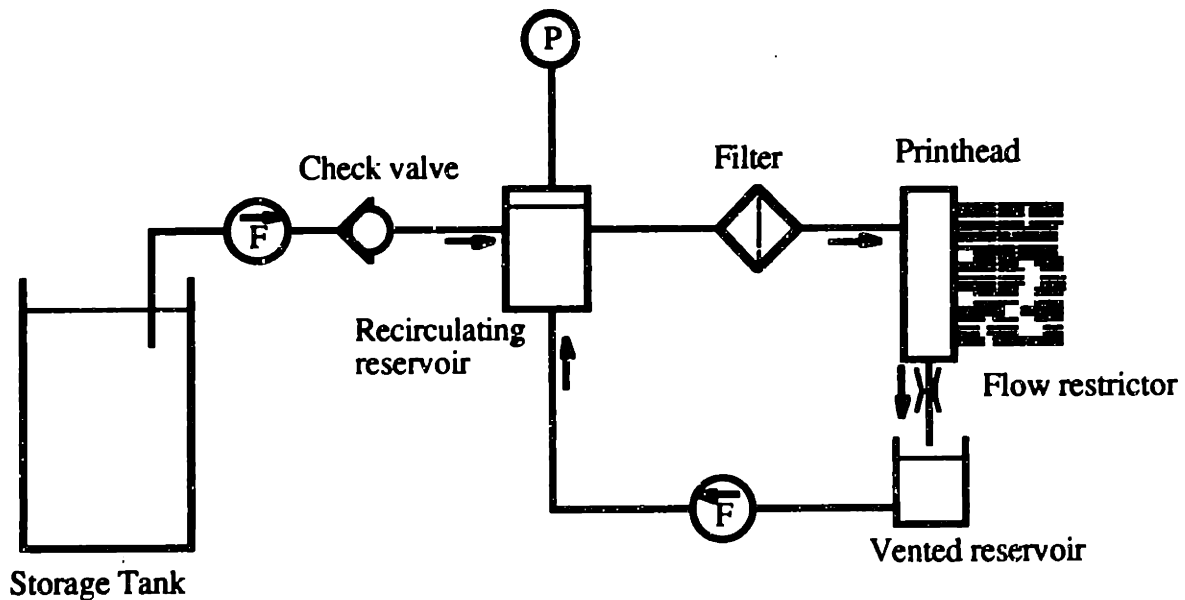


Figure 5.6a: Cross-flushing system using two flow sources and one pressure source.

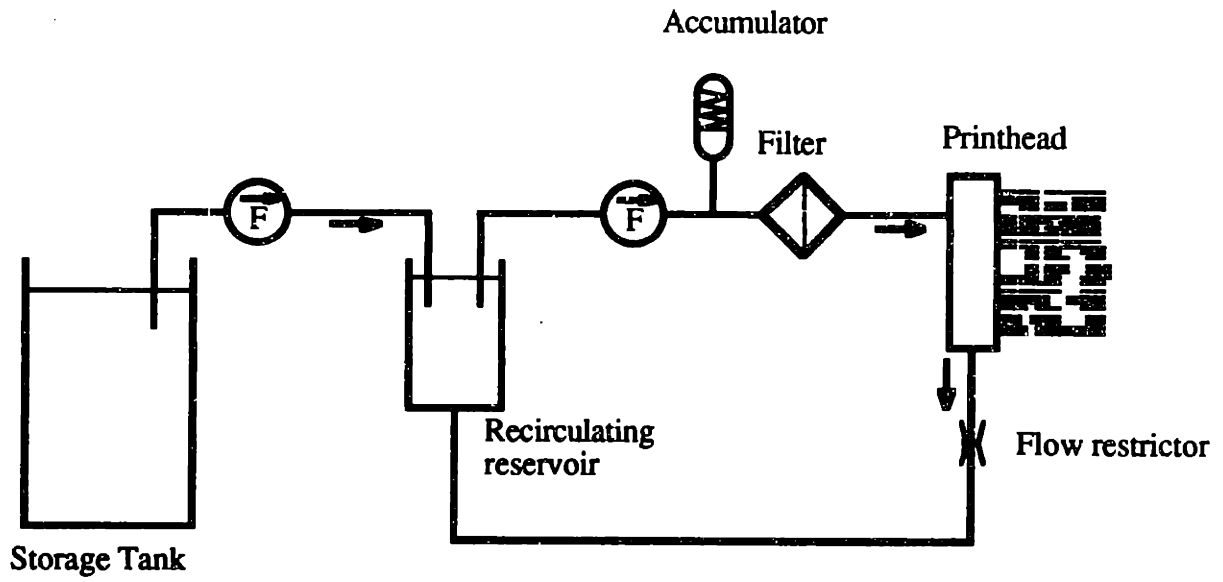


Figure 5.6b: Cross-flushing system using two flow sources.

## References

- Bahl, Surinder, Research and Development, Eastman Kodak Co., Dayton, Ohio. Private communication on Aug. 24, 1990.
- Bredt, Jim "Physics of our Printhead," Three Dimensional Printing group literature, April 1991.
- Brongo, Diane, Engineering Consultant, Boston, MA. Electronic circuit design, December 1990, March 1991.
- Curry, S.A. and H. Porig, "Scale Model of an Ink Jet," *IBM J Res Dev*, vol. 21, no. 1, 1977, pp. 10-20.
- Drake, D.J. et al., "A Novel Continuous Ink Jet Drop Generator," *The Third International Congress on Advances in Non-Impact Printing Technologies*, Society for Imaging Science and Technology, VA, August 1986, pp. 276-283.
- Fagerquist, Randy, Research and Development, Eastman Kodak Co., Dayton, Ohio. Product information.
- Fillmore, G.L. et al., "Drop Charging and Deflection in an Electrostatic Ink Jet Printer," *IBM J Res Dev*, vol. 21, no. 1, 1977, pp. 37-47.
- Heartling, Gene H. (Motorola Inc.) "Piezoelectric and Electrooptic Ceramics"
- Heinzl, J. and Hertz, C.H., "Ink-Jet Printing," *Advances in Electronics and Electron Physics*, vol. 65, p. 91.
- Hertz, C.H. and Samuelsson, B., "Ink Jet Printing of Photographic Quality Color Images," *The Fourth International Congress on Advances in Non-Impact Printing Technologies*, Society for Imaging Science and Technology, VA, March 1988, pp. 196-202.
- Hertz, C.H. and Samuelsson, B., "High Quality Ink Jet Printing of Color Images," *The Third International Congress on Advances in Non-Impact Printing Technologies*, Society for Imaging Science and Technology, VA, August 1986, pp. 231-238.
- Hermanrud, B. and Hertz, C.H., "Ink Jet Development at the Lund Institute of Technology," *Journal of Applied Photographic Engineering*, vol. 5, no. 4, Fall 1979, pp. 220-225.
- Horowitz, P. and Hill, Winfred, "The Art of Electronics, 2nd ed.," Cambridge University Press, NY 1989.
- Keterberg, J.A., "Drop Charging and Deflection using a Planar Charge Plate," *The Fourth International Congress on Advances in Non-Impact Printing Technologies*, Society for Imaging Science and Technology, VA, March 1988, pp. 241-249.
- Knittel, P., ed., "A Selected Bibliography on Ink Jet Printing," Technical and Education Center of the Graphic Arts, Rochester Institute of Technology, NY, 1981.

- Lee, F.C. et al., "Drop -On-Demand Ink Jet Printing at High Print Rates and High Resolution," *Advances in Non-Impact Printing Technologies for Computer and Office Applications*, Gaynor, J. ed., Van Nostrand Reinhold, NY, June 1981, pp. 1059-1070.
- Levanoni, M., "Study of Flow through Scaled-up Ink Jet Nozzles", *IBM J Res Dev*, vol. 21, no. 1, 1977, pp. 56-68.
- Minto, G.S., "The Domino Unijet Ink Jet Printer," *Advances in Non-Impact Printing Technologies*, Gaynor, J. ed., Van Nostrand Reinhold, NY, June 1981, pp. 1051-1058.
- Piezo Kinetics, Inc., Bellafonte, PA. Company literature.
- Piezo Systems, Inc., Cambridge, MA. Company literature.
- Phinney, R.E. and Humphries, W., "Stability of a Laminar Jet of Viscous Liquid-Influence of Nozzle Shape," *American Institute of Chemical Engineering Journal*, vol. 19, 1973, pp. 655-657.
- Pimbley, W.T. "Drop Formation from a Liquid Jet: A Linear One-Dimensional Analysis...", *IBM J Res Dev*, vol. 20, no. 12, March, 1976, pp. 148-155.
- Pimbley, W.T. and Lee, H.C. "Satellite Droplet Formation in a Liquid Jet," *IBM J Res Dev*, vol. 21, no. 1, 1977, pp. 21-30.
- Rezanka, I. and Crowley, J.M., "Satellite Control by Direct Harmonic Excitation," *The Third International Congress on Advances in Non-Impact Printing Technologies*, Society for Imaging Science and Technology, VA, August 1986, pp. 284-295.
- Spehrley, Corky, Research and Development, Spectra, Inc., Hanover, N.H. Site visit. March 28, 1991.
- Stone, J.J., "The New Technology of Videojet Systems," *Advances in Non-Impact Printing Technologies*, Gaynor, J. ed., Van Nostrand Reinhold, NY, June 1981, pp. 1032-1050.
- Turner, Ron, Research and Development, Piezo Kinetics Inc., Bellafonte, PA. Private communication on April 9, 1991.
- Williams, Paul, "Three Dimensional Printing: A new Process to Fabricate Prototypes Directly from CAD Models," M.I.T. Masters Thesis, May 1990.
- Yamada, T. et al., "Microdot Ink-Jet Printer," *Advances in Non-Impact Printing Technologies*, Gaynor, J. ed., Van Nostrand Reinhold, NY, June 1981, pp. 978-990.

# **Appendix 1: Piezo Operation**

## **A1.1 Introduction**

This Appendix is intended to provide a basic understanding of piezo function and to apply this information to the design of a piezo configuration for use with Three-Dimensional Printing.

Piezoelectricity is defined as "electric polarization produced by mechanical strain in crystals belonging to certain classes; the polarization being proportional to the strain and changing with it [Heartling]. Two main phenomena are observed: the "direct effect" whereby electric charge, or polarization, is generated from a mechanical stress, and the "inverse effect," in which an applied electric field can generate mechanical movement. Therefore, these materials can be used either as generators or motors. We will only concern ourselves with the inverse effect.

Piezoelectricity can only occur in ceramic materials with crystallographic structures lacking a center of symmetry (a necessary condition for the formation of electric dipoles). A mechanical stress, which causes relative motion between positive and negative ions, produces an electric dipole. Likewise, creating an electric dipole will cause relative motion between ions.

Since crystallites are randomly oriented in a ceramic material, no piezoelectric effects will be observed unless the material is "poled" under an electric field. This process orients dipoles within individual crystallites roughly in the direction of the electric field. After poling, the ceramic behaves much like a single crystal. We shall see that the direction of poling directly effects the behavior of the piezoelectric material ("piezo" for short).

## A1.2 Quantifying piezo behavior

The state equations describing generator and motor behavior, respectively, are

$$D = dT + e^T E \quad (1)$$

$$S = s^E T + dE \quad (2)$$

Where:

- D is polarization,
- S is the strain,
- E is electric field strength,
- T is stress,
- d is a piezoelectric coefficient,
- s is the material compliance, and
- e is the dielectric constant.

Directional properties are specified using subscripts as indicated in figure A1.1.

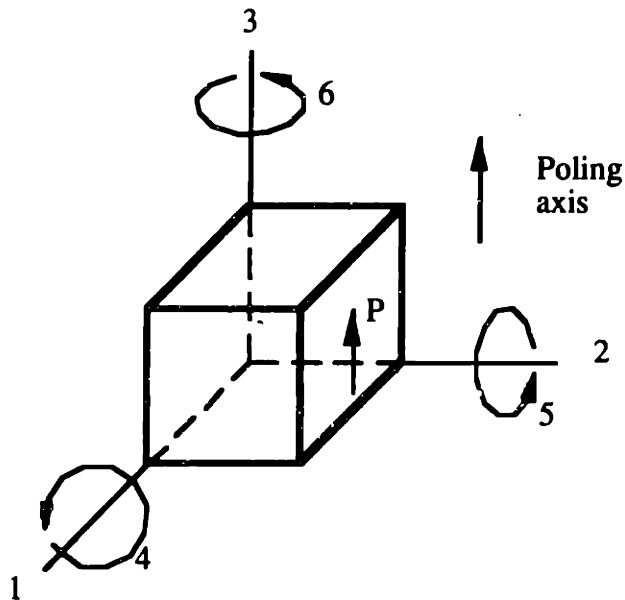


Figure A1.1: Subscript conventions for piezo materials.

The 3 direction is parallel to the poling direction, while directions 1 and 2 are orthogonal and the 4,5, and 6 subscripts are used to represent shear. The polarization vector "P" points from the positive to the negative poling electrode. Coefficients have two subscripts; the first indicates the direction of the electric field relative to the poling axis; the second relates to mechanical stress or strain. A superscript indicates a boundary condition.

These are:

- T: constant stress; not mechanically constrained.
- S: constant strain; mechanically clamped.
- E: constant field; short-circuit.
- D: constant electrical polarization; open-circuit.

There are several important coefficients which are described below.

#### Charge coefficients

The coefficients  $d_{31}$ ,  $d_{33}$ , and  $d_{15}$  are proportionality constants between strain and electric field, or between polarization and stress, according to the relationship

$$d = \frac{S}{E} = \frac{D}{T} \quad (\text{meters per volt}).$$

$d_{33}$  applies when strain is measured in the same direction as the electric field.  $d_{31}$  refers to strain measured orthogonal to the electric field, and  $d_{15}$  indicates shear produced about the 2 axis when an electric field is applied in the 1 axis.

Materials with a large  $d_{ij}$  will have relatively large mechanical displacements for a given voltage, generally a desirable characteristic for motor applications.

#### Voltage coefficients

The  $g_{ij}$  coefficients measure the ratio of electric field to mechanical stress, and is related to the  $d$  coefficient via the dielectric constant according to

$$g = \frac{d}{K\epsilon_0} = \frac{E}{T} = \frac{S}{D}.$$

$d = Ke_0 * g$  is essentially the formula  $Q=CV$ , reflecting the fact that below their natural frequency, piezos behave like capacitors. High  $g$  coefficients are desirable where high voltage outputs are desired as a result of mechanical stress, such as phonograph pickups.

#### Coupling coefficients

The  $k_{ij}$  coupling coefficient measures the ability of a piezoceramic to convert one form of energy to another. It is defined as the square root of the ratio of available mechanical energy per electrical energy input. Since this is a measure of efficiency, values are always less than unity. The coefficient  $k_p$  refers to planar or thin disk (radial) energy conversions (.72 is typical for the PZT material), while  $k_t$  refers to thickness coupling.

### **A1.3 Mechanical deformations**

Typically, deformations are on the order of a few microns in piezo motors. This can be increased several orders of magnitude by using a "bimorph," whereby two piezo plates are glued together in such a way that when stimulated, one will contract while the other expands. The unit then assumes the surface of a sphere, but for many applications can be treated as a beam in bending. Typical configurations are shown in figure A.2.



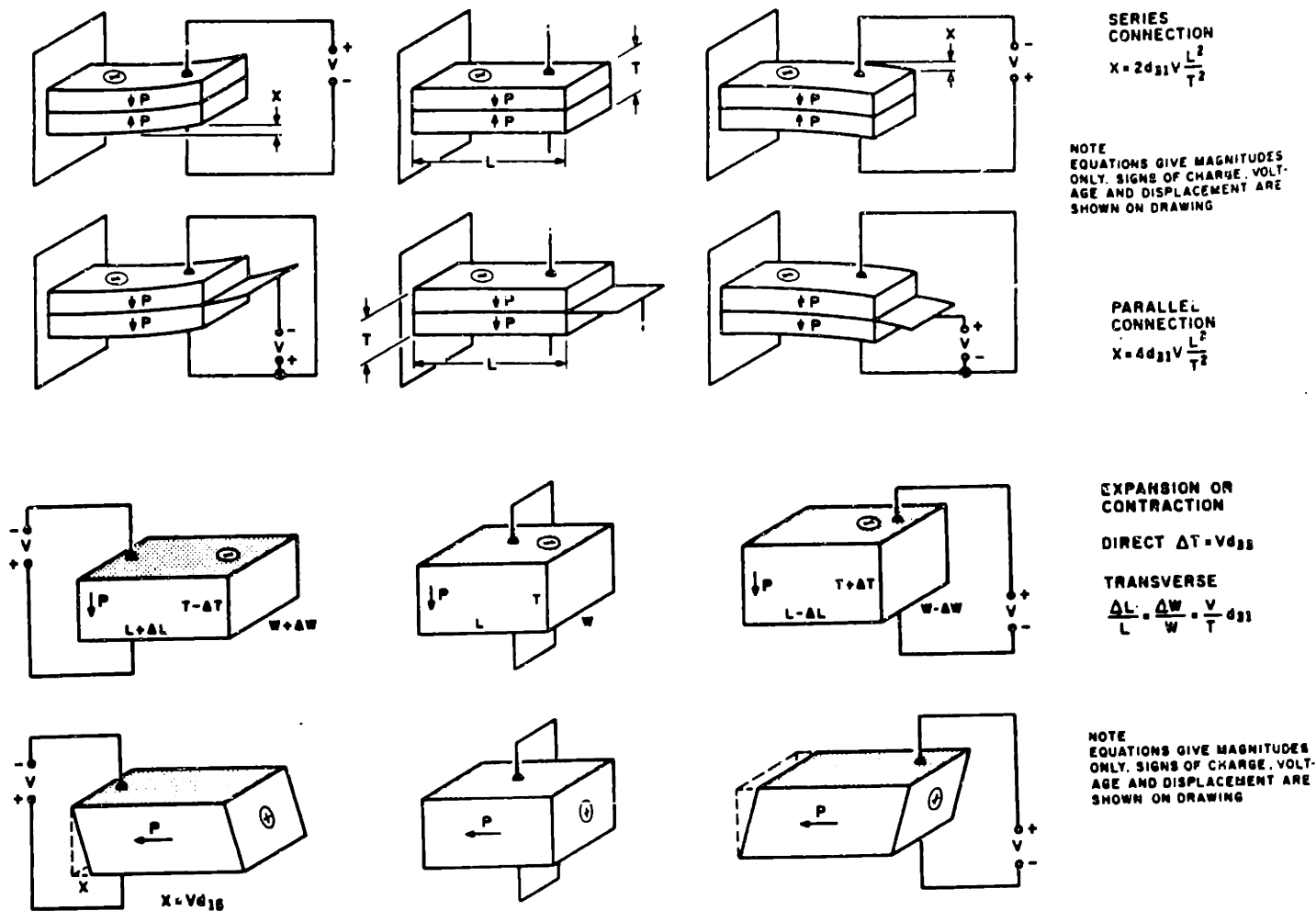


Figure A1.2: Stimulation modes for piezo motors [Piezo Systems].

For example, let us calculate the movement of a thin disk .51 mm thick and 4.78 mm in diameter (the outside dimensions of the piezo disk currently used on the nozzle assembly).

$$d_{33} = \frac{S}{E} = \frac{\Delta t}{t(V/t)} = \frac{\Delta t}{V}$$

$$\Delta t = d_{33}V.$$

Note that movement is independent of disk/plate thickness. Taking  $d_{33} = 300 \times 10^{-12}$ , a 100 volt signal produces a change of

$$\Delta t = 300 \times 10^{-12} \text{ m/V} \times 100 \text{ V} = .03 \text{ } \mu\text{m} = 1.1 \text{ } \mu\text{in.}$$

In the radial direction, we have

$$d_{31} = \frac{s}{E} = \frac{\Delta r}{r(V/t)} = \frac{\Delta r t}{rV}$$

$$\Delta r = d_{31} \frac{rV}{t}$$

Taking  $d_{31} = -125 \times 10^{-12} \text{ m/V}$  and using a 100 volt signal, we compute

$$\Delta r = 125 \times 10^{-12} \text{ m/V} \times \frac{4.78 \times 10^{-3} \text{ m}}{5.1 \times 10^{-4} \text{ m}} \times 100 \text{ V} = .12 \text{ } \mu\text{m} = 4.6 \text{ } \mu\text{in.}$$

Here we see that radial motion is dependent on plate dimensions.

## Appendix 2: Charging Characteristics of Printhead and Nominal Parameters

### A2.1 Charged droplet behavior in an electrostatic field

Inside the charging cell, a droplet accumulates a charge per unit mass of

$$\frac{q}{m} = \frac{C'V_1u}{\dot{m}} \quad [\text{Bredt}].$$

Here,  $V_1$  is the charging cell voltage,  $u$  is stream velocity, and  $\dot{m}$  is mass flow rate.  $C'$  is the capacitance per unit length of the parallel-plate arrangement with a fluid stream acting as a central terminal, given by

$$C' = \frac{2\pi\epsilon_0}{\ln\frac{d_1}{d} + k} = \text{Capacitance per unit plate length.}$$

A charged droplet is acted on by a force  $F = qE = ma_x$  where  $E$  is the electric field inside the deflection cell. Then

$$a_x = \frac{q}{m} \frac{V_2}{d_2} = \frac{C'V_1V_2u}{\dot{m}d_2}$$

Since the acceleration on a droplet is determined by its charge/mass ratio and the electric field it experiences, the characteristics of the charging and deflection cells play an equal role in determining the path of a charged droplet. The following equation can be derived [Bredt] for the horizontal distance  $x_d$  that the stream can be expected to deflect at a distance  $l_3$  away from the bottom of the deflection cell (see figure A2.1):

$$x_d = \frac{a_x}{u^2} \left[ \frac{1}{2} l_2^2 + l_2 l_3 \right]$$

From the above equations, we see that acceleration increases with  $V_1$  and  $V_2$ , and decreases with distance between deflection plates  $d_2$  and the log of  $d_1$ . The following characteristics are desired:

- Minimized charge on each droplet.

Highly charged droplets tend to repel each other, interfere with uncharged droplets, and, at an extreme, atomize. Additionally, higher voltages are more difficult to modulate.

- Maximized distance between charging plates.

This makes the printhead more robust to stream error and eases setup.

- Deflection plates held some minimum distance apart.

This prevents buildup from bridging the gap and sparking.

- Low deflection voltage.

Sparking becomes more common as this voltage approaches 3000 volts.

Since the optimal values of these four factors (which have been listed in order of importance) are fighting each other, some compromise must be made. The easiest compromise is simply to accept a lower acceleration force. This results in milder curvature for droplets and effectively lengthens the printhead, which in turn increases the distance between the nozzle tip and the part. While one would expect this to result in poorer part accuracy due to aerodynamic noise, the visible effects of even a one inch increase are small (although this has not been studied at any length). Therefore, at this stage this is a logical relaxation in the printhead constraints, and results in improved reliability.

## A2.2 Nominal parameter values

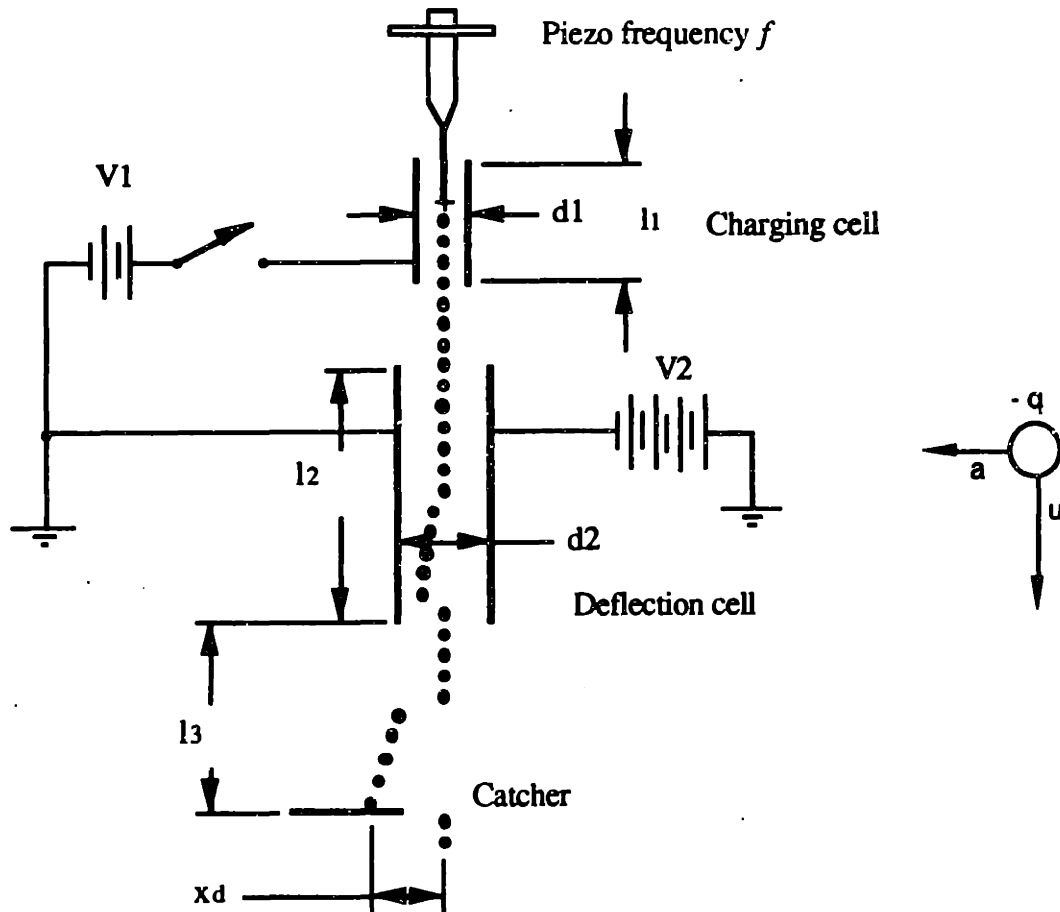


Figure A2.1: Physical representation of parameters.

### Charging Cell

$V_1 = 120$  volts (causes droplets to be negatively charged)

$d_1 = .026$ " (spacing between charging plates)

$l_1 = .250$ " (length of charging cell)

### Deflection Cell

$V_2 = -1000$  to  $-3000$  volts, 2500 volts nominal (Voltage on high-voltage plate)

$d_2 = .050$ " (distance between deflection plates)

$l_2 = .320$ " (length of high-voltage plate)

$l_3 = .240$ " (distance from base of high-voltage plate to catcher)

## Fluid Jet

$u = 10\text{-}14$  m/sec, 12.4 m/sec nominal (jet velocity)

(m/sec) =  $10.16 \frac{\text{m}^3}{\rho}$  (ml/min) (flow rate)

$f = 30\text{-}100$  kHz., 50 kHz. nominal (droplet generation frequency)

$d = .003$ " nominal (droplet diameter- a function of  $f$  and  $u$ )

## Derived Quantities for nominal operating conditions

$C' = 25$  pF/m

$q/m = 1.5 \times 10^{-3}$  coulombs/kg

$x_d = 1.28 \times 10^{-5}$  m/V \*  $V_1 = 1.5 \times 10^{-3}$  meter @ 120 volts.

$V_2/d_2$  (max) =  $2 \times 10^6$  V/m (observed dielectric breakdown of air)

## Appendix 3: Partial Droplet Charging

The electronic circuit responsible for modulating a signal to the charging cell must convert a square wave TTL signal into a square wave signal switching from 0 to up to 120 volts. This output ( $V_1$ ) is applied to the charging plates.

The charge on each droplet is determined by the charging cell voltage at the instant in which breakoff occurs. Ideally,  $V_1$  will always be either 0 or 120 volts, so droplets will either be fully charged or completely uncharged. However, due to unwanted capacitances, a square wave input will not produce a square wave output.  $V_1$  will therefore have intermediate values. A typical response curve to a square wave input is shown below.

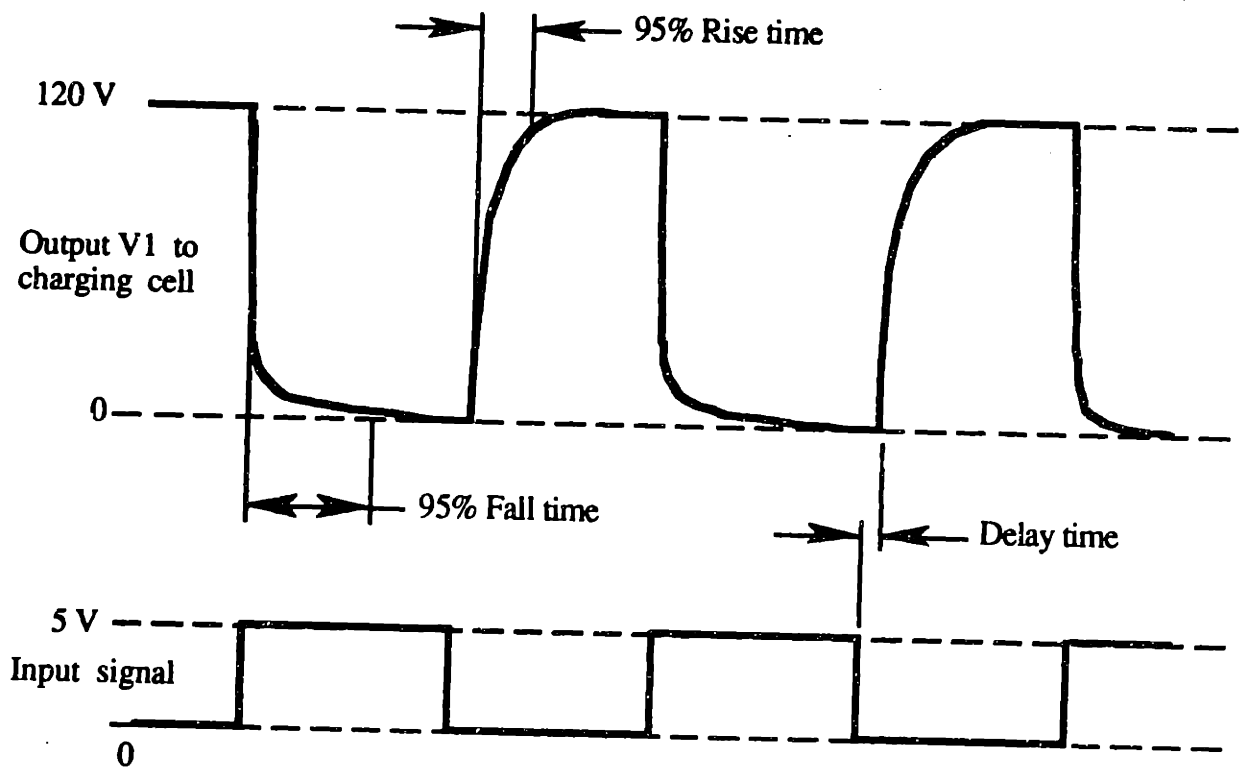


Figure A3 1: Response of  $V_1$  to a 40 kHz square wave input signal

Figure A3.1 shows how the signal would respond to a square wave at approximately 40 kHz. The square wave is simulating the computer output during part production; in

actuality the signal would be neither this fast nor this regular. Typically the 95% rise time is on the order of 5  $\mu\text{s}$ , and the 95% fall time is far higher (around 50  $\mu\text{s}$ ). The 99% fall time is up around 200 $\mu\text{s}$ !

If a droplet breaks off while  $V_1$  is at an intermediate value, it will receive a charge proportional to that voltage. There are two possible cases, both of which may result in a misplaced droplet.

**Incomplete deflection.**

Note that when droplet generation is driven at 50 kHz., a droplet is produced every 20  $\mu\text{s}$ . Consequently, depending on the relationship between the input signal and the piezo frequency, the occurrence of incompletely charged droplets is likely.  $V_1$  must only pass some threshold in order for droplets to be charged enough to deflect onto the catcher plate. However, the time it takes to rise to this threshold must be reduced to decrease the likelihood of incomplete charging. The piezo signal frequency and phase could potentially be synchronized to the input signal in such a way that incomplete charging can be avoided.

**Unwanted deflection.**

The opposite situation, in which  $V_1$  falls exponentially towards zero volts, is of greater concern since any nonzero voltage can cause proportional deflection.  $V_1$  appears to fall very quickly ( $< 1\mu\text{s}$ ) to within a few volts of zero, however it takes the output far longer, up to several hundred microseconds, to drop to within one volt. This situation is acceptable for now but the "next generation" circuitry should force this voltage to go to zero.

The current circuit design (figure 3.5) attempts to minimize rise and fall time through the choice of a (supposedly) fast transistor, appropriate values of resistance and capacitors to minimize RC constants, and Schottky diodes which are meant to prevent transistor saturation and have the effect of reducing the delay time (figure A3.1). The rise time of  $V_1$ , which corresponds to the time it takes to shut off the transistor, is very dependent on capacitances in the circuit and external wiring. Disconnecting the wires leading to the



charging cell, for example, decreases the 98% rise time from 5 $\mu$ s to 2 $\mu$ s. (Our goal for the next circuit is under 1  $\mu$ s.)

The easiest way to improve circuit performance is to design the printhead to function with a lower charging voltage! This will decrease rise and fall times and permit the use of faster components.

# **Appendix 4: Satellite Droplets**

## **A4.1 Introduction**

The difficulties associated with satellite droplet formation are not unique to Three Dimensional Printing. Researchers in the ink-jet printing field have written numerous papers on the subject of understanding and controlling this phenomenon, indicating that this industry suffers from these problems as well. In spite of this, however, no satisfactory solution seems to have yet been reached. Authors propose techniques or a set of conditions in which satellites will not form or are unlikely to form, but none of them are robust to changes in parameters that would be varied during normal operation [Curry, Portig; Pimbley; Pimbley, Lee; Rezanka, Crowley]. One research effort has found an interesting solution to this problem - they print using only the satellite droplets! [Yamada et al.] Although the literature does not present any clear solutions, it aids in understanding satellite formation and suggests several directions for study and experimentation with binder. This work is summarized below.

## **A4.2 Studies of satellite droplet formation**

Attempts to model satellite behavior have at best provided a qualitative feel. Linear models of unstable jets do not predict satellite formation and most non-linear models predict satellites all the time, although the elimination of these droplets is observed under certain conditions [Pimbley, Lee]. Pimbley and Lee, however, developed a second order nonlinear model using spatial instability which predicted several modes of satellite formation over a certain domain. This model gives good qualitative results, but requires still higher order terms for a more quantitative description of the process.

Satellite droplets are formed between the main droplets as an unwanted side-effect of periodic perturbation of the jet. Typically, the jet will develop a narrow neck between

growing droplets just prior to breakoff (figure A4.1, A4.2). This neck develops into a satellite droplet as it detaches from adjacent droplets at points A and B and snaps back to form a sphere. This interaction is critical because momentum transfer can occur during the time that only one breakoff has occurred, resulting in a relative velocity between the satellite and the main drops. There are at least five possible cases:

(1) Breakoff occurs at point B before it occurs at point A. While the necked region is still attached at A, surface tension begins pulling it towards the trailing droplet. Breakoff then occurs at A, resulting in a satellite droplet which is moving towards the trailing droplet. The two droplets merge a short distance downstream. This "rearward merge" condition is the most common.

(2) Breakoff occurs at point A before it occurs at point B. While the necked region is still attached at B, surface tension pulls it towards the leading droplet. Breakoff then occurs at A, resulting in a satellite which moves toward the leading droplet and "forward merges" downstream.

(3) Breakoff occurs nearly simultaneously at points A and B. As a result, no momentum is transferred, and the satellite never merges.

(4) Breakoff occurs only at point B. Surface tension pulls the necked region into the trailing droplet before breakoff can occur at A. As a result, a satellite is never formed.

(5) Breakoff occurs only at point A, and the necked region is sucked into the leading droplet before breakoff can occur at A. Again, no satellites are formed.

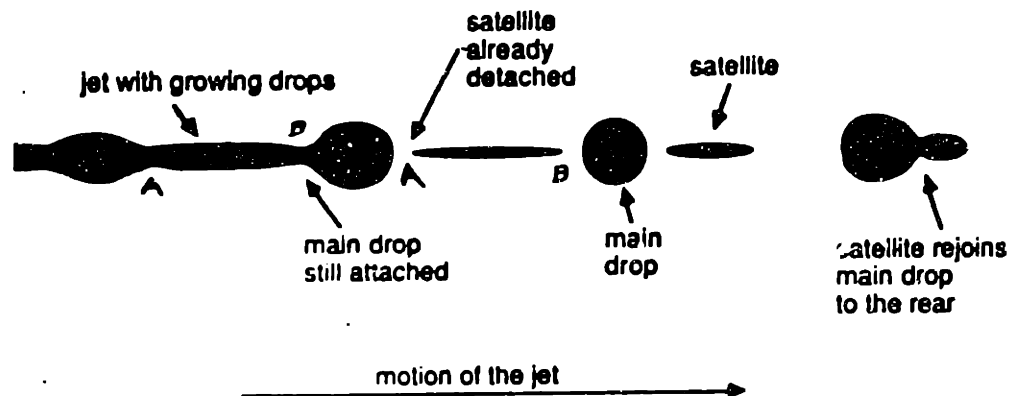


Figure A4.1: Typical rearward merging satellite droplet behavior.



Figure A4.2: Photograph of satellite droplet formation in a binder jet.

The ratio of droplet wavelength to jet diameter ( $\lambda/d$ ) is also important in determining satellite formation. When  $\lambda/d$  is between 5 and 7, it is claimed that cases (4) and (5) from above can be achieved [Pimbley, Lee]. If this ratio is too high, larger main droplets and long necked regions will make cases (1) through (3) more likely. At a low ratio, drop spacings are small and separation occurs rapidly at both ends.

Authors agreed that satellite formation is influenced by combinations of driving frequencies or harmonics of the fundamental frequency. According to Pimbley's nonlinear theory, an initially sinusoidal perturbation waveform would develop into a wave which

included the harmonic frequencies. Resonant waves at these different frequencies would form a beat frequency envelope on the stream. The characteristics of drop formation would depend on how the beat frequency envelope matched the travelling waves at the drop separation point. The formation of satellite drops would be either suppressed or enhanced by this interaction [Pimbley].

Rezanka and Crowley have achieved control over satellite formation by exciting a stream using independent control over the amplitude and phase of several harmonics. The proper combinations can produce regimes for a given flow rate and fundamental frequency where no satellites will occur. However, These regimes change substantially as frequency is varied, and it is unclear how phase and amplitude parameters for satellite-free operation can be predicted. Typically, stream velocity must be held to +/- 3% to remain in this range.

In another study, a 50:1 scale model was used to study droplet breakoff behavior on a large scale [Curry, Portig]. A number of parameters were varied to establish operating conditions for a "print window" for satellite-free printing. The following results were obtained over a limited range of operating conditions (and should therefore be considered cautiously):

- Satellite-free conditions exist only between a minimum and a maximum piezo excitation voltage (the "print window").
- The print window always occurred at  $\lambda/d$  ratios between 4 and 7.
- The print window was increased at lower Reynolds and Weber numbers. This corresponds to fewer satellites at reduced density and increased surface tension and viscosity.
- A square wave with a 40% high duty cycle had a much greater print window than a sinusoidal signal at one set of conditions.
- The print window shifted upwards at low temperatures (16 degrees C) and downwards at high temperatures (38 degrees C), suggesting that less energy was transferred from the piezo to the stream at low temperatures.
- Sharp-edged orifices had poorer performance than rounded orifices under certain conditions.

## A4.2 Implications for Three Dimensional Printing

The behavior of satellite droplets from a binder jet and their dependence on parameters such as piezo configuration, amplitude, frequency, flow rate, and viscosity are not well understood. From our observations, their existence is most strongly dependent on frequency, and satellites are observed to nearly vanish at certain frequencies using certain "efficient" nozzles (nozzles which transmit the most piezo energy to the stream).

With a  $46\mu$  nozzle at typical parameters of a 1.25 cc/min binder flow rate and a piezo frequency of 70 kHz., the printhead may be "tuned" by slightly varying this frequency to run with very few satellites at a  $\lambda/d$  ratio of only 3.8. The discrepancy between this value and the recommended ratio of 5 to 7 may be a result of the different properties of binder.

Most of the experimental results presented above would be fairly easy to reproduce for the binder stream. Adding harmonics to the excitation signal and experimenting with different binder properties (viscosity, surface tension, density) and temperature might yield some interesting results. Additives, such as a visco-elastic material that would alter droplet breakoff, could be tried.

## **Appendix 5: Printhead Evolution**

Printhead design occurred over several months, and could be described as "rocky." At first, the goal was "it should switch the stream on and off" but it soon became clear that those words are synonymous with "it can't short, clog, spark, sputter, flood, or destroy expensive equipment," to name only a few special requirements.

The major impediment to this early research is that the designs weren't robust to the many things that could go wrong. The development process consisted of taking on these problems one by one and steadily increasing robustness and reliability.

### **A5.1: Overall concept development**

The initial apparatus was very simple and consisted of a nozzle holder, a ground plate, a graphite plate with a hole drilled thru to serve as a charging cylinder, and a high voltage plate. At best, some 50 percent of the time it could be made to deflect a binder stream on to the ground plate at least once. Flooding, shorting, and clogging nozzles were the most pervasive problems. The hole was very small, at .015" diameter, and the stream error was frequently large enough to cause the stream to intercept the graphite. Shorting occurred frequently because there were many locations where collecting fluid could cause a current path. There was no mechanism for removing deflected binder.

A set of modifications were made which included drilling the hole out to .022," carving out material around the high voltage plate to impede shorting, and adding an "irrigation" system, shown in figure A5.1. A new ground plate was built with a narrow slot, a water supply line, and a suction line. Water was directed down through the slot and sucked away at the bottom. Deflected droplets landed in the groove and were whisked away by the stream. Suction was provided by an aspirator pump.

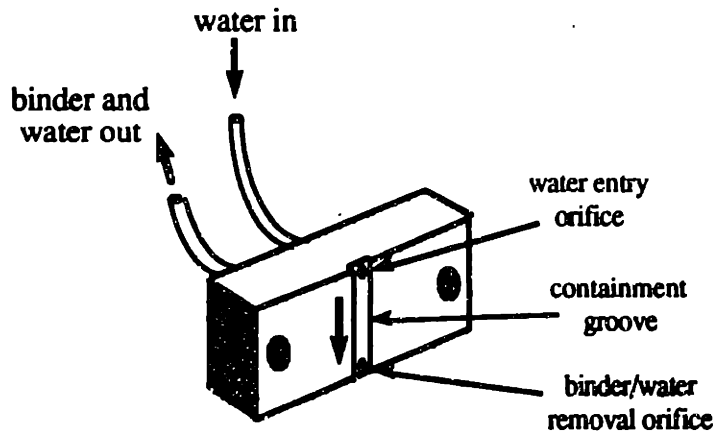


Figure A5.1: Droplet removal system for prototype printhead.

The droplet removal system worked fairly well, but the aspirator worked marginally well and the suction line repeatedly clogged with binder. Shorting and sparking still occurred, and liquid buildup was collecting on the high-v plate. The printhead was still very difficult to run. A new apparatus, shown in figure A5.2, was built with the following characteristics:

- isolated charging cylinder to minimize possibility of shorting
- easy removal or modification of charging ring
- made provisions for neat electrical connections
- added view-ports to study stream deflection
- added suction ports for two major flooding locations to recover from floods.
- mountable to machine





This was the first modular design, as it allowed the charging cylinder and nozzle holder/locator to be removed from the printhead body. This allowed experimentation with different lengths and diameters for the charging cell, and varying distances between the nozzle tip and the charging cell. The design of the plexiglas body made shorting less likely, since "live" components were better shielded from each other. A BNC connector eliminated much of the cluttersome wiring, and a functional switching circuit was built at this point, so this design could conceivably be used to print parts. The printhead succeeded in deflecting binder and appeared to function successfully with a 10 KHz. square wave input. However, it was still not nearly reliable enough.

While the suction ports did significantly aid nozzle startup, they could not effect recovery from all floods, the suction lines clogged from the binder, and they did nothing to eliminate the cause of the flooding. Shorting still occasionally occurred, and stream angle error was still causing floods.

To contend with the stream error, the nozzle tip was mounted in a drilled out teflon ball and a pivot arm was built onto the printhead support. This allowed the user to adjust the nozzle angle with a set screw to compensate for error. This made the printhead more complicated but was a step forward in reliability. The aluminum high voltage plate was replaced by a thin copper plate mounted in a teflon holder to further minimize the possibility of shorting. In recognition of the fact that starting nozzles with binder was a bad thing to do since it almost guaranteed to make a mess out of the printhead, a binder/water switch was added upstream of the nozzle and it was made common practice to run for several minutes with water before switching to binder.

With these modifications, a "tic-tac-toe" board was successfully printed. The part took about two hours to print. This was a crucial stepping stone, as it was the first demonstration of the ability to print parts using a switching printhead, and an important measure of the

ultimate success of the 3-D Printing process. Overcoming this obstacle allowed some breathing room, and time to think about a new, more reliable design.

The current prototype is intended to satisfy the criteria listed in section 3.1. One significant improvement is an "external frame" configuration, where the aluminum body is far removed from the stream path, compared to a solid block with internal components which became a disaster when it flooded. In the event of a flood, the wet components can simply be removed, cleaned, and replaced to eliminate the problem.

Another significant change is the use of charging plates rather than a charging cylinder. While charging plates charge somewhat less efficiently than a cylinder, they are far more robust to errors in stream angle, since sensitivity to errors in one axis are relaxed completely.

Furthermore, the "slot" design of the charging assembly permits nozzle startup without any danger of flooding. During startup, the narrow slot is removed completely until the stream has been stabilized and centered. Startup failures, a serious problem with previous models, are very rare with the current design.

## **A5.2: Droplet catcher design- the continuing story.**

While the "irrigated channel" ground plate and droplet catcher was functional, it was suboptimal because:

- it requires a suction pump and a water supply
- the suction line becomes clogged with binder
- unprinted binder cannot be recycled
- spray causes fluid buildup on the high-v plate.

A simpler mechanism was sought for droplet catching and removal. The criteria are as follows:

- catches deflected droplets cleanly
- eliminates collected drops cleanly

- requires minimum deflection of droplets
- easy to clean
- reasonably simple and easy to construct
- robust to:
  - stream error
  - varying droplet deflection angle
  - flow rate
  - cycle time for traverse
- minimizes distance from nozzle to part

It was realized that the printhead could be simplified if droplet removal was accomplished using a stationary system rather than something which moved with the printhead. Therefore the idea of a "service station," which would sit at one end of printhead travel and collect droplets at the end of each pass, was developed. This service station could potentially clean the printhead as well, or provide vending machines and roadmaps.

A new ground plate/catcher configuration used a "knife edge" to direct deflected droplets towards a horizontal area where a drop of binder would form. At the end of each pass, the printhead would "dock" with a fixed structure which used capillary action to collect the drop from the catcher plate. The collected drop then drained down a tube into a bottle. Binder that collected in this bottle could be recycled for later use.

This configuration worked fairly well. However, there were two problems. The first was that the collection structure, which used a brush or "moustache" to collect fluid, eventually became clogged up with dried binder. However, with the printhead in its current orientation, it was realized that the inertia of the binder drop on the moving printhead was enough to fling it off the catcher at the end of each stroke, where accelerations are highest. Thus, the moustache was eliminated and a nylon "bathtub" was placed at each end of travel into which drops would be tossed and then drain into a recollection tank. This configuration was successful and is used on the current machine.

The second problem was that during use, the knife edge would collect a blob of binder buildup which would grow in size until it interfered with printhead operation, usually causing

it to flood. This problem was caused by partially charged droplets which could not deflect far enough to clear the knife edge and instead accumulated on it (due to slow transistor response- see Appendix 3).

While one logical approach to tackling this problem was to improve the electronic circuitry that is causing the problem, another approach was to design a droplet catcher that was robust to the problem. Both approaches were taken, but the second approach resulted in two new configurations in which the knife edge was eliminated altogether. These are shown in figure 3.4 and discussed in section 3.3.5. In both designs, partially charged droplets cannot interfere with printhead operation, as they print into the powder rather than the printhead. Since these errant droplets are relatively few, they have very minor effects on a typical printed part.

## Appendix 6: Parts Drawings

### PRINTHEAD PARTS LIST

<u>QTY</u>	<u>PART OR DRAWING</u>	<u>MATERIAL</u>
1	PRINTHEAD BODY	ALUMINUM
1	NOZZLE PIVOT ARM	ALUMINUM
1	TEFLON NOZZLE CLAMP	NYLON
1	3/16" x 3/4" DOWEL PIN	STEEL
1	CHARGING CELL HOLDER	DELTRIN
1	CHARGING CELL	ALUMINUM
1	HIGH VOLTAGE ASSEMBLY	EPOXY, STEEL ELECTRODES
1	GROUND PLATE HOLDER	ALUMINUM

# PRINthead BODY

3-D PRINTING GROUP

3/27/91

DRAWN BY DAVE BRANCAZIO

253-2606 (DAY)

253-5028 (MESSAGE)

864-3214 (HOME)

ALL DIMENSIONS IN  
INCHES. TOLERANCES:

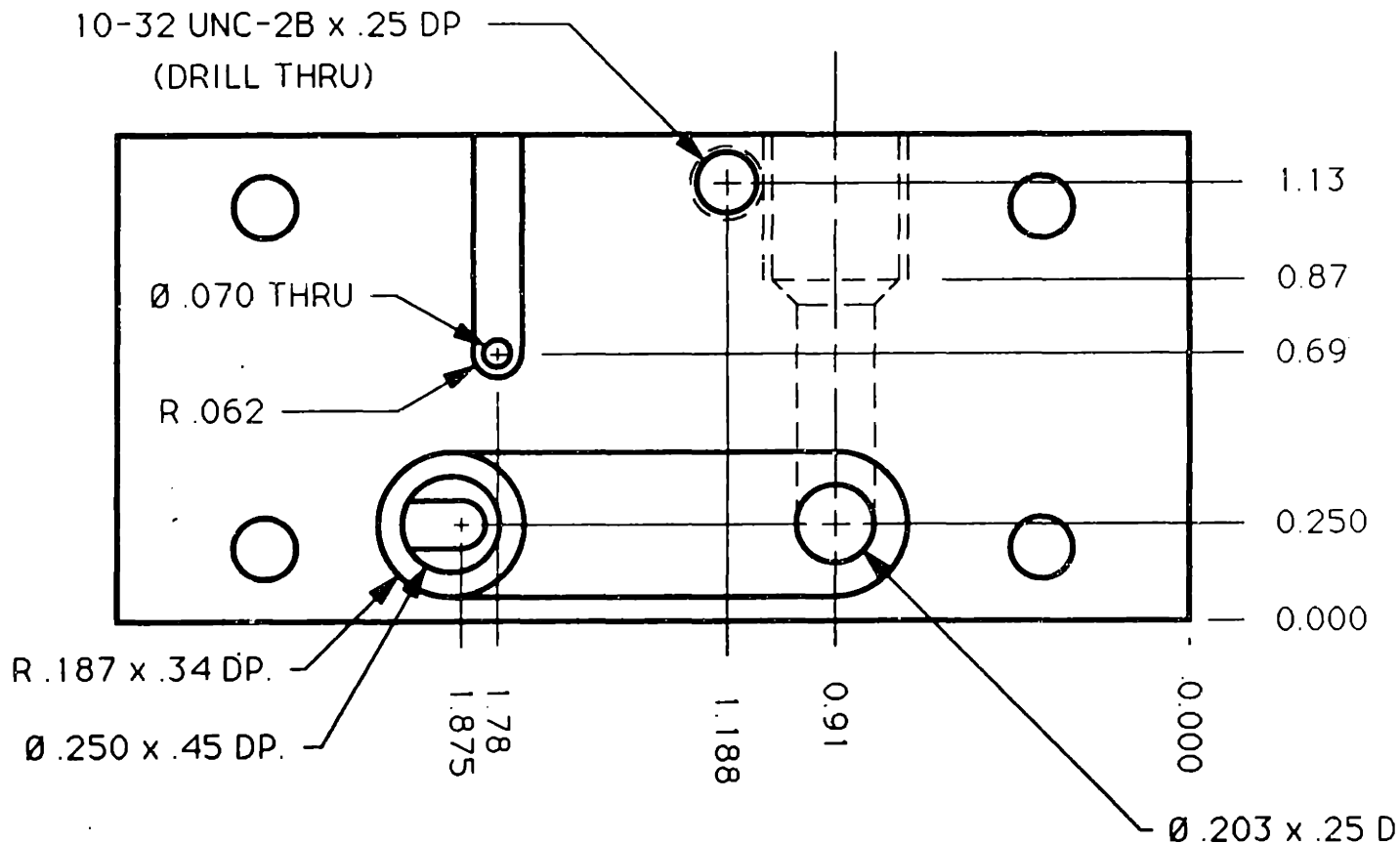
X.XXX =  $\pm 0.001$

X.XX =  $\pm 0.005$

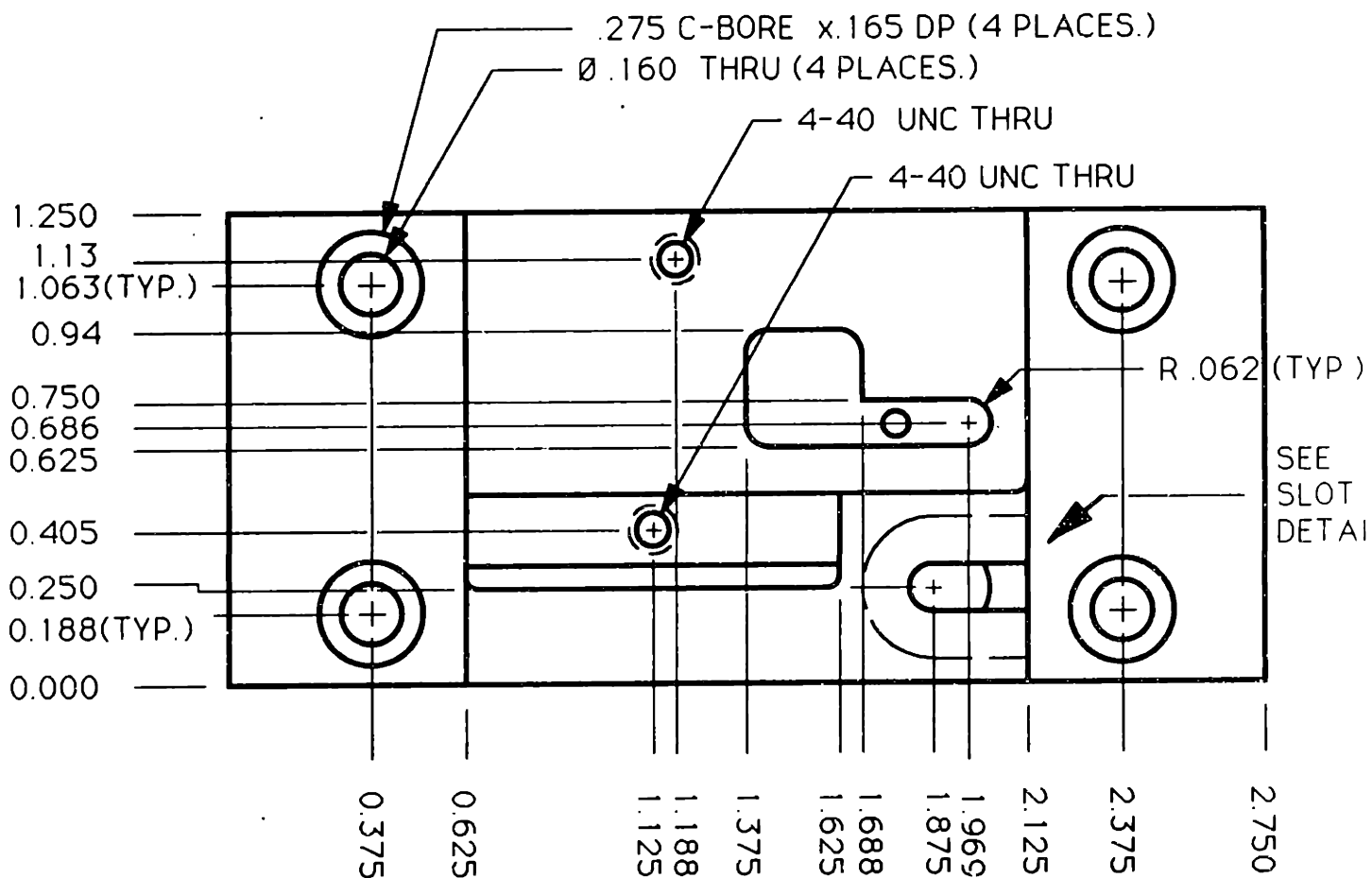
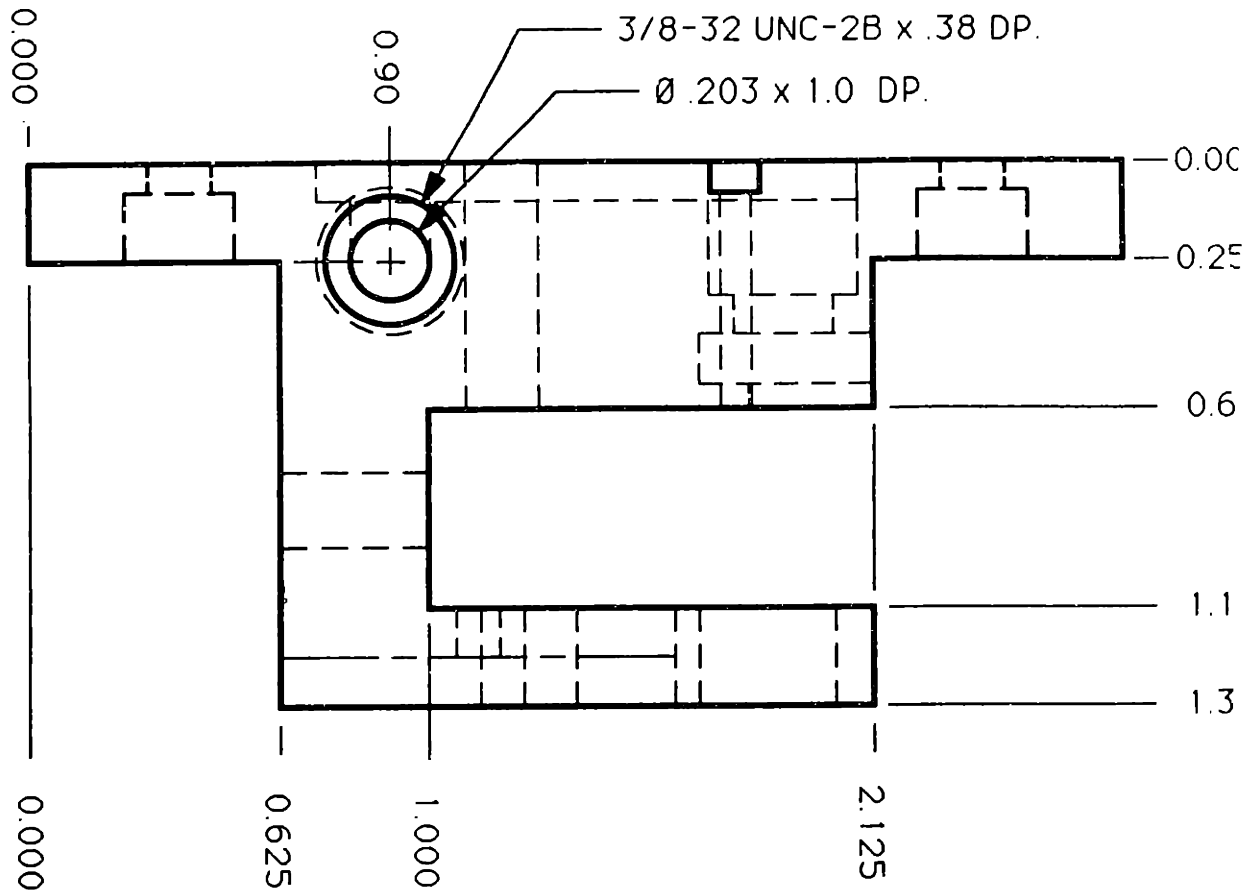
X.X =  $\pm 0.02$

SCALE 2:1

MATERIAL: 6061-T6 ALUMINUM



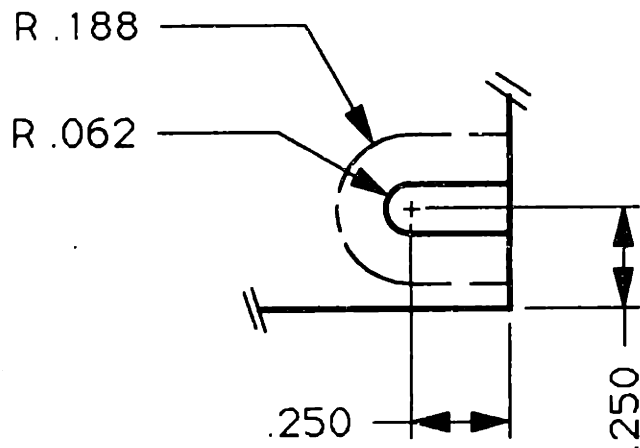
NOT ALL HIDDEN LINES SHOWN



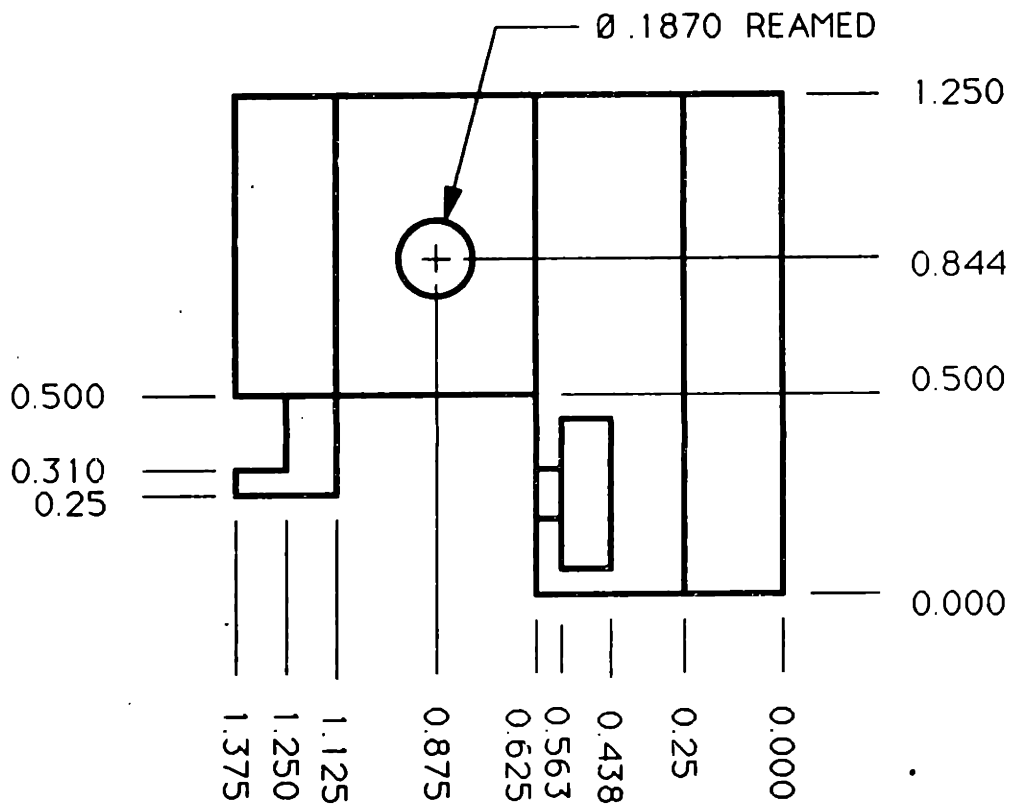
NOT ALL HIDDEN LINES SHOWN- SEE SECTION VIEWS



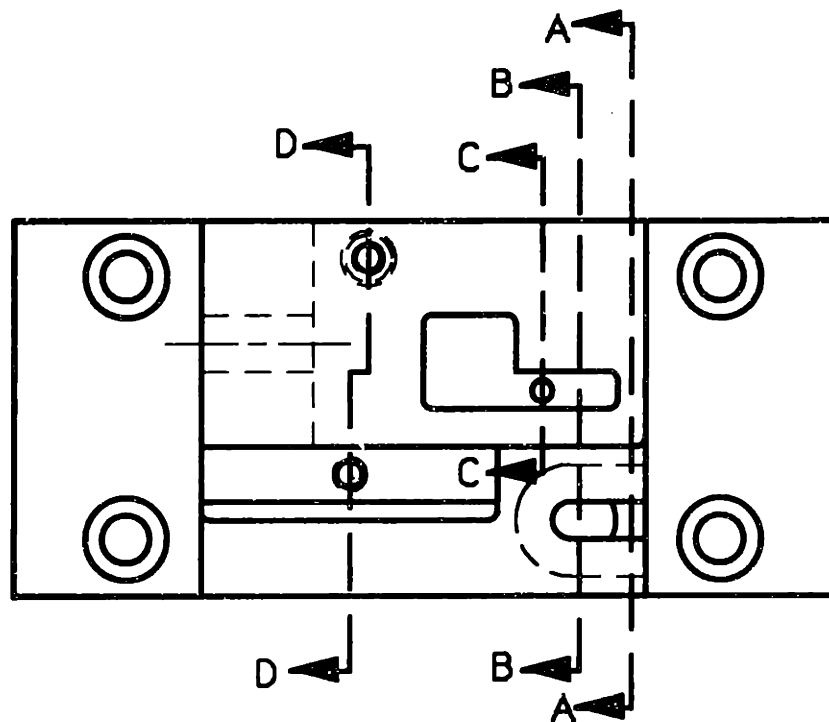
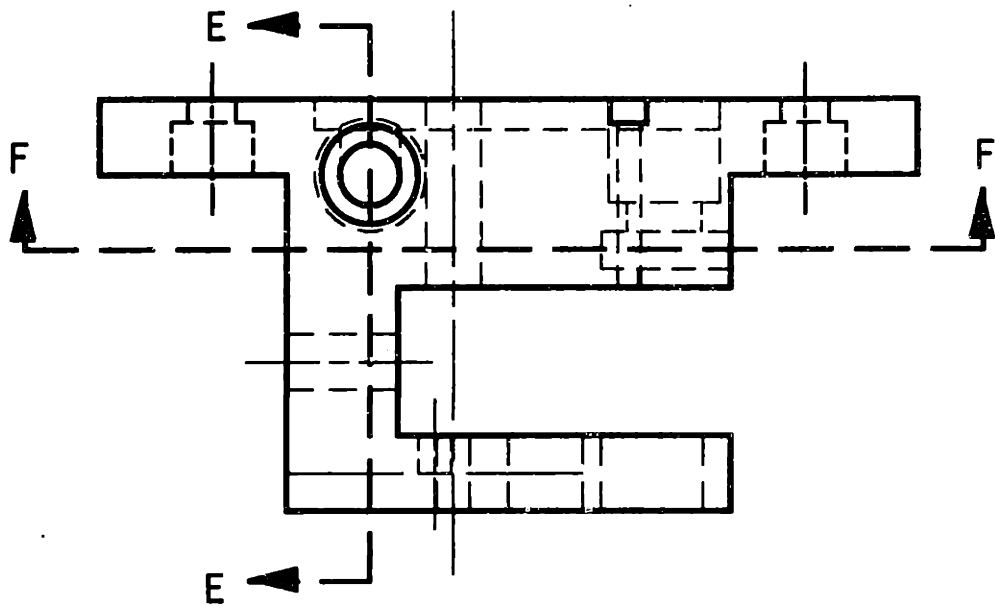
SLOT DETAIL



USE .388 x .125 WOODRUFF CUTTER  
TO MAKE SLOT

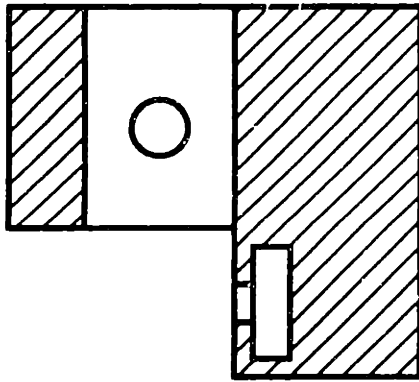


HIDDEN LINES NOT SHOWN- SEE SECTION VIEWS

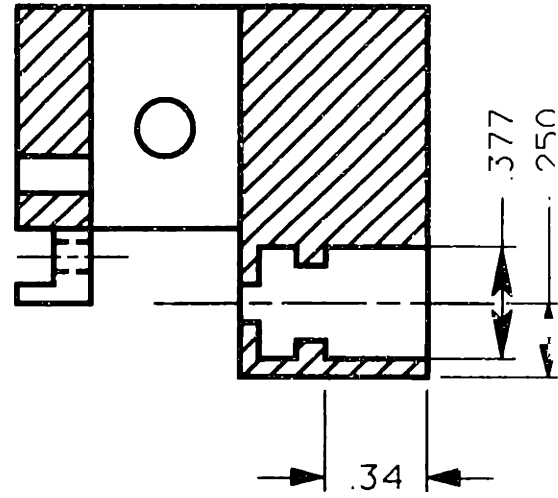


SECTION LEGEND  
SCALE 1.5 : 1

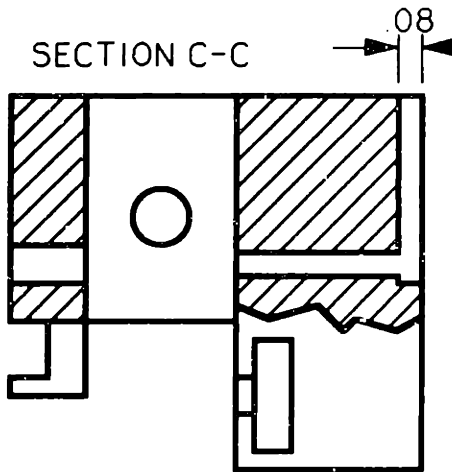
SECTION A-A



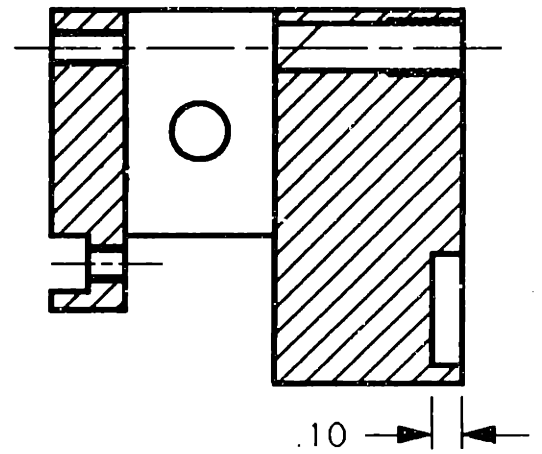
SECTION B-B



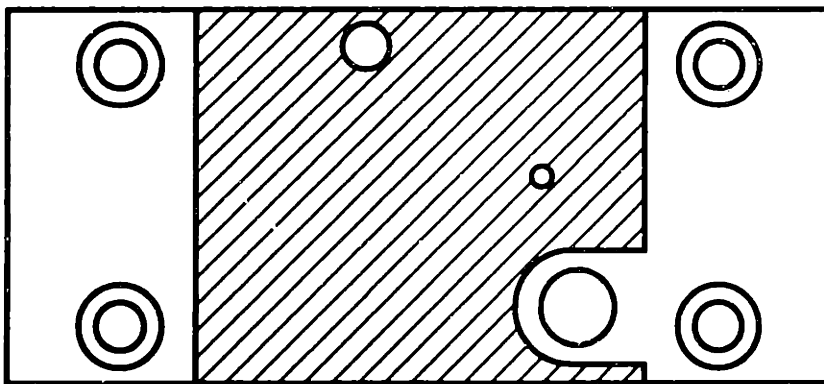
SECTION C-C



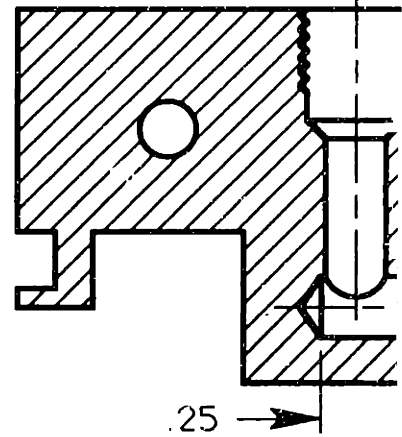
SECTION D-D



SECTION F-F

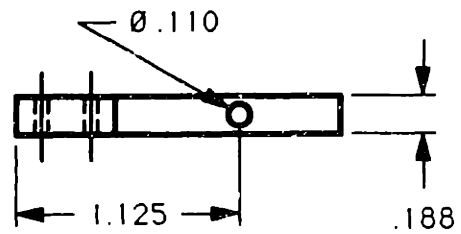
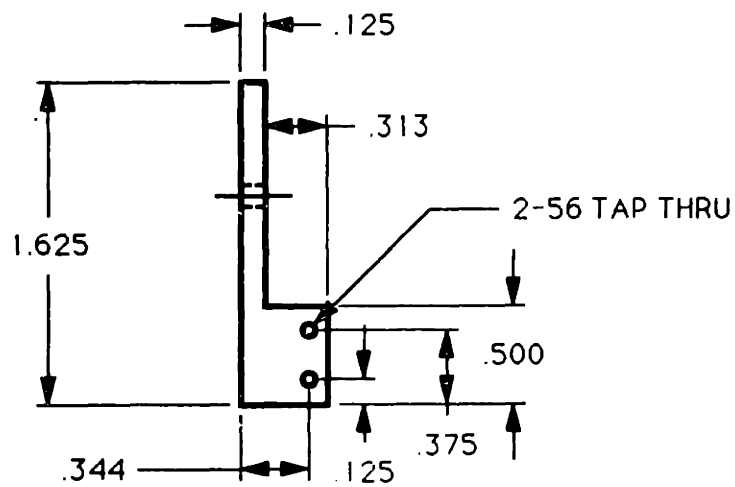


SECTION E-E



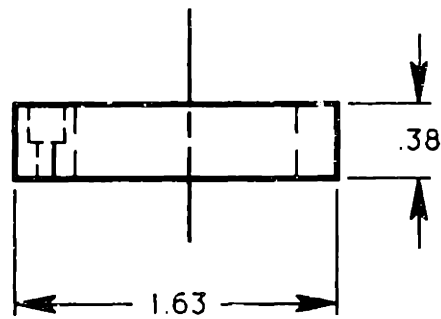
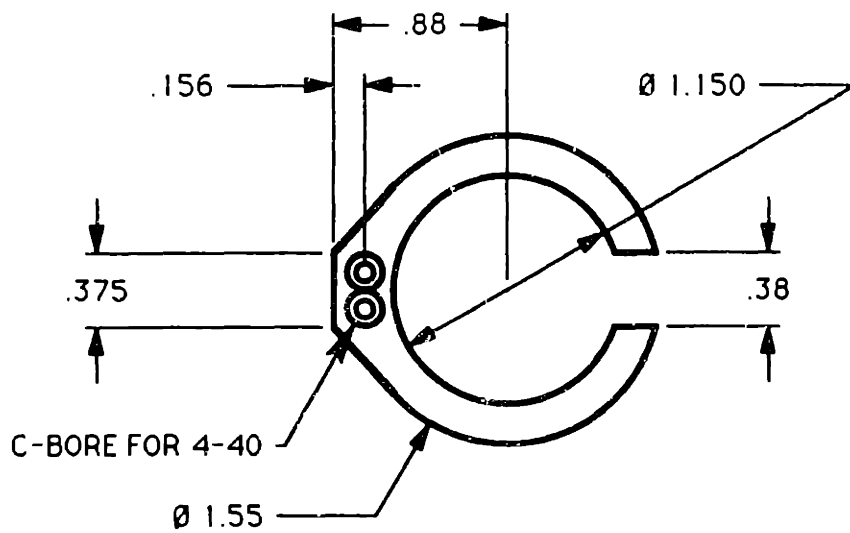
SCALE 1.5 : 1

HOLE INTERSECTION  
DETAILS NOT  
IMPORTANT



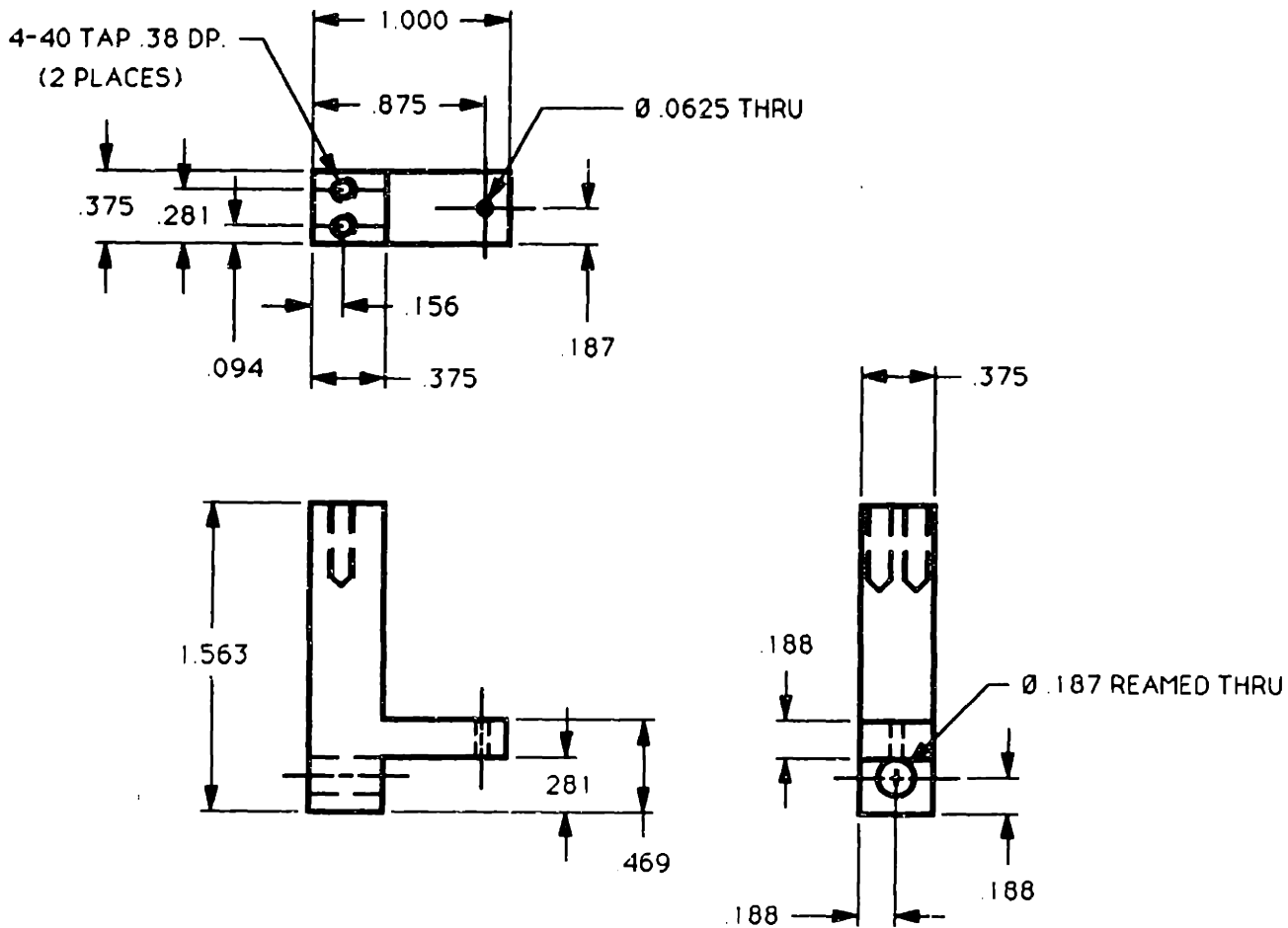
GROUND PLATE HOLDER  
 DRAWN BY BRANCAZIO 4/7/91  
 SCALE 1:1

ALL DIMENSIONS  
 IN INCHES.  
 TOLERANCES:  
 X.XXX = ±.001  
 X.XX = ±.005  
 X.X = ±.02



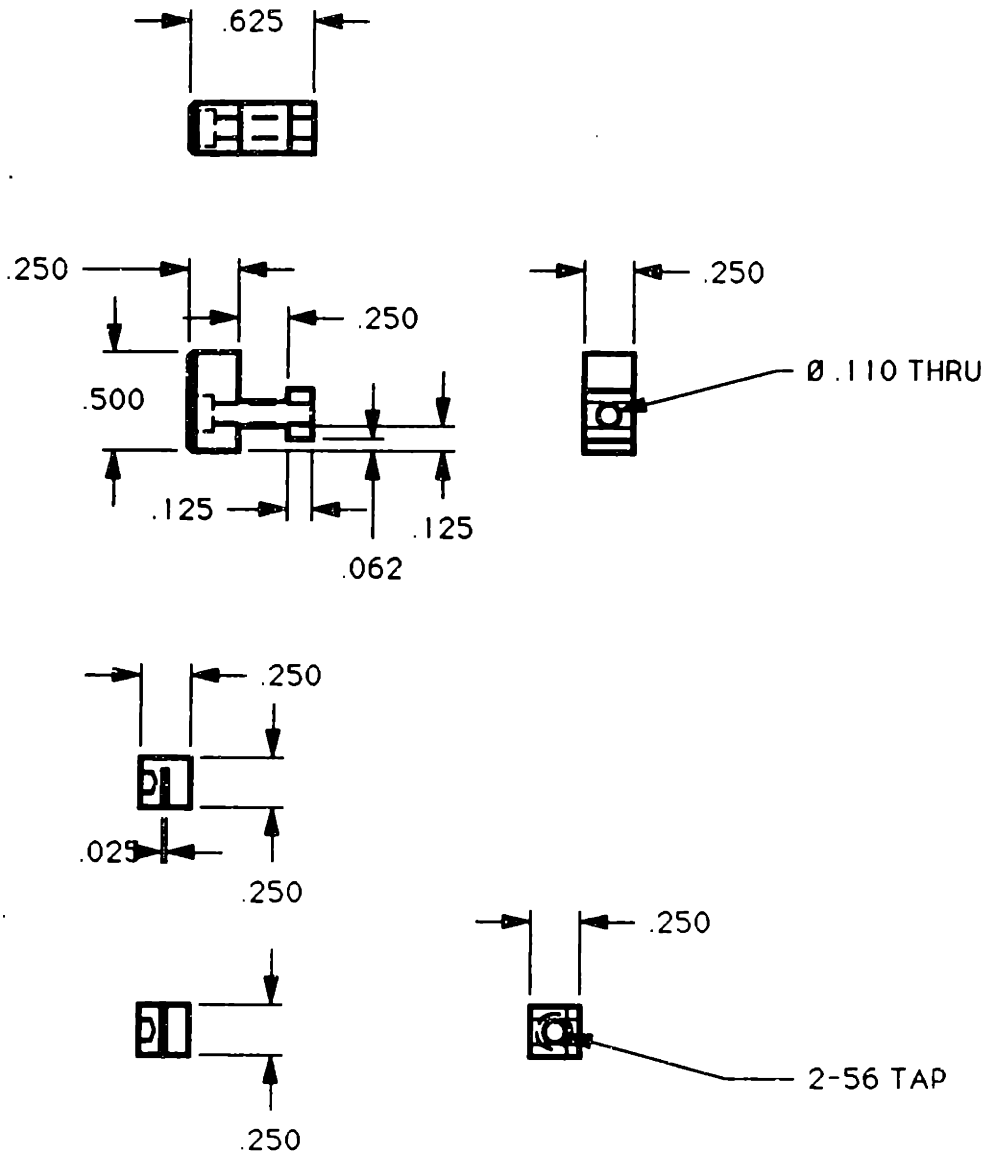
NOZZLE ASSEMBLY CLAMP  
 DRAWN BY BRANCAZIO 4/7/91  
 SCALE 1:1

ALL DIMENSIONS  
 IN INCHES.  
 TOLERANCES:  
 X.XXX = ±.001  
 X.XX = ±.005  
 X.X = ±.02



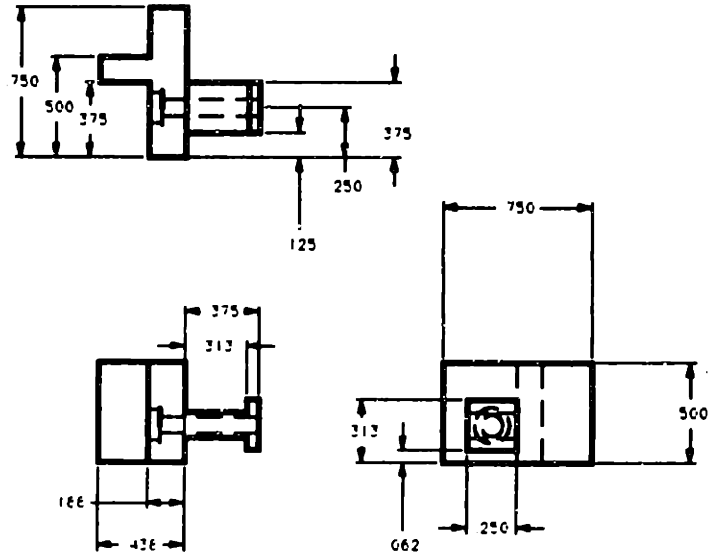
NOZZLE ASSEMBLY PIVOT MOUNT  
 DRAWN BY BRANCAZIO 4/7/91  
 SCALE 1:1

ALL DIMENSIONS  
 IN INCHES.  
 TOLERANCES:  
 X.XXX = ±.001  
 X.XX = ±.005  
 X.X = ±.02



CHARGING CELL ASSEMBLY  
 DRAWN BY BRANCAZIO 4/7/91  
 SCALE 1:1

ALL DIMENSIONS  
 IN INCHES.  
 TOLERANCES:  
 X.XXX =  $\pm .001$   
 X.XX =  $\pm .005$   
 X.X =  $\pm .02$



NEW CHARGING CELL HOLDER  
 DRAWN BY BRANCAZIO 4/7/91  
 SCALE 1:1

ALL DIMENSIONS  
 IN INCHES.  
 TOLERANCES:  
 X.XXX =  $\pm 0.001$   
 X.XX =  $\pm 0.005$   
 X.X =  $\pm 0.02$